# Detailed Study of the $^4$He Nuclei through Response Function Separations at High Momentum Transfers

K. Aniol (spokesperson), M. Epstein, and D. Margaziotis

*California State University, Los Angeles, CA 90032, USA*

W. Bertozzi, Z. Chai, S. Gilad (spokesperson),
D.W. Higinbotham (spokesperson), M. Rvachev, S. Sirca, R. Suleiman,
Y. Xiao, X. Zheng, J. Zhou, and Z. Zhou

*Massachusetts Institute of Technology, Cambridge, MA 02139, USA*

J.P. Chen, E. Chudakov, J. Gomez, J.-O. Hansen, C.W. de Jager,
S. Jeschonnek, B. Reitz, J. LeRose, A. Saha (spokesperson) [1], and
B. Wojtsekhowski

*Jefferson Lab, Newport News, VA 23606, USA*

J.-M. Laget

*Centre d'Etudes de Scaclay, Gif-sur-Yvette, France*

C.F. Perdrisat

*College of William and Mary, Williamsburg VA 23187, USA*

P. Markowitz

*Florida International University, Miami, FL 33199, USA*

E. Cisbani, F. Cusanno, F. Garibaldi, S. Frullani, M. Iodice, and
G.M. Urciuoli

*INFN, Laboratorio di Fisica, I-00161 Rome, Italy*

J. Mougey, P. Moussiegt, E. Penel, G. Quemener, and E. Voutier

*Institut des Sciences Nucléaires, Grenoble, France*

P.E. Ulmer and L. Weinstein

*Old Dominion University, Norfolk, VA 23529, USA*

X. Jiang

*Rutgers, Piscataway, NJ 08854, USA*

E. Piasetzky
*Tel Aviv University, Tel Aviv, Israel*

Z.-E. Meziani
*Temple University, Philadelphia, PA 19122, USA*

W. Korsch
*University of Kentucky, Lexington, KY 40506, USA*

K.G. Fissum
*University of Lund, Box 118, SE-221 00 Lund, Sweden*

C.C. Chang and J.J. Kelly
*University of Maryland, College Park, MD 20742, USA*

J. Calarco
*University of New Hampshire, NH 03824, USA*

A. Hotta
*University of Massachusetts, Amherst, MA 01003, USA*

D. Day R. Grima R. Lindgren B.E. Norum B. Sawatzky A. Stolin K. Wang
*University of Virginia, Charlottesville, VA 22901, USA*

---

**Abstract**

We propose a detailed study the electromagnetic structure of $^4$He through (e,e'p) coincidence measurements at high momentum transfers. In perpendicular kinematics, this will be accomplished by measuring the quasi-elastic $^4$He(e,e'p)$^3$H cross section at a fixed $\mathbf{q} = 1.50$ GeV/c and $\omega = 0.84$ GeV as a function of missing momentum up to 1.2 GeV/c. We shall also extract the response function $R_{TL}$ and the left-right asymmetry $A_{TL}$ up to $p_m = 0.5\ GeV/c$, and extract $R_T$ and $R_{L+TT}$ for missing momenta around 0 GeV/c, 0.4 GeV/c, and 0.5 GeV/c. These measurements will provide detailed observables to test current and future theoretical models. In parallel kinematics, we shall study the $Q^2$ dependence of the reaction $^4$He(e,e'p)$^3$H by performing a longitudinal/transverse $R_L/R_T$ separation from protons emitted along $\mathbf{q}$ in the $Q^2$ range from 0.81 to 4.1 [GeV/c]$^2$ with missing momenta near zero. We shall also make $R_L/R_T$ separations of the reaction $^4$He(e,e'p)pnn for high missing momentum, $p_m = 0.3$ GeV/c, for a $\mathbf{q}$ of 1.0 GeV/c to investigate nucleon-nucleon interactions. These measurements will be performed in Hall A, using the two high resolution spectrometers and a cryogenic $^4$He target. Hall A is the only facility in the world where such measurements can be performed.

---

[1] contact person: A. Saha, phone: (757) 269-7605, e-mail: saha@jlab.org

**Contents**


1 Overview of Goals 4

2 Kinematics 6

3 Physics Motivation 8

4 Relation to other Jefferson Lab Proposals 18

5 Experimental Setup 20

6 Theoretical Predictions 28

7 Expected Results 31

8 Beamtime Request 39

References 40

## 1 Overview of Goals

We propose to study the structure and electromagnetic currents in $^4$He using the $^4$He(e,e'p) reaction. We intend to concentrate on aspects which can be uniquely measured in Hall A, namely those related to short-distances in the nucleus. In particular, we intend to measure the $^4$He(e,e'p)$^3$H cross section up to missing momentum of about 1.2 GeV/c, and to separate response functions in regions where their sensitivity to the various nuclear currents can provide an important means for understanding the measured observables. In certain kinematics, the large momentum acceptance of the spectrometers will be used to also obtain data in the missing-energy continuum.

The proposed measurements can be divided into "perpendicular" (non-parallel) and parallel kinematics (see Section 2 for details). The perpendicular kinematics are suitable for measuring the cross sections up to very high missing momentum and is needed for the separation of the longitudinal-transverse interference response, $R_{TL}$, and the left-right asymmetry $A_{TL}$. It is also possible to separate the transverse response, $R_T$, and a combination of the longitudinal and transverse-transverse interference responses, denoted in this proposal as $R_{L+TT}$. All observables can be measured with the same transfered momentum and energy, hence fixed kinematic conditions. In parallel kinematics, a unique separation of $R_L$ and $R_T$ can be obtained. However, because of the constraint imposed by fixing the angle between the transfered momentum and the ejected proton, varying the missing momentum requires varying either the transfered momentum or energy, resulting in significant changes in kinematic conditions.

We shall use perpendicular kinematics to measure the $^4$He(e,e'p)$^3$H cross section at quasi-elastic kinematics for missing momentum, $p_m$, in the range 0 GeV/c to 1.20 GeV/c by varying the angle between the transfered momentum $\mathbf{q}$ and the ejected protons. This will be done at fixed electron kinematics: a fixed beam energy of 4.80 GeV, a fixed three-momentum transfer $\mathbf{q}$ of 1.50 GeV/c, and fixed energy transfer of 0.840 GeV. This will extend substantially the set of available data which currently extend only to $p_m$ = 0.690 GeV/c [1,2] which were obtained in various kinematics due to the limitations of the facility; whereas our measurements will be performed in quasi-elastic kinematics. In addition, it is predicted that our proposed measurements at much higher transfered momentum and energy (and hence high ejected-proton energies) provide better handles on effects such as final-state interactions (FSI) and meson-exchange currents (MEC).

For the missing momentum range 0 GeV/c to 0.500 GeV/c, we shall measure also the $R_{TL}$ response and the $A_{TL}$ asymmetry. This is done by measuring the cross sections for ejected protons on both sides of the transfered momentum vector. $R_{TL}$ and $A_{TL}$ have been shown to be less sensitive to FSI than the cross section, while being more sensitive to ingredients such as relativistic dynamics and the current operator [3]. These observables will provide important additional constraints to modern model calculations currently being developed.

Finally, for missing momentum of around 0 GeV/c, 0.400 GeV/c, and 0.500 GeV/c, we

shall perform additional measurements at the same transfered momentum and energy, but at different beam energies (and hence electron angle and virtual-photon polarization). This will enable the separation of $R_T$ and $R_{L+TT}$ responses in bins of 25 MeV/c between 0.325 and 0.575 GeV/c. All models predict a dip in the cross section in this $p_m$ range, which was not observed in measurements at NIKHEF [2] nor in recent Jefferson Lab measurements [4]. We hope that the three measured responses and the $A_{TL}$ asymmetry will provide enough details to understand what fills the predicted minimum.

In parallel kinematics we shall perform a Rosenbluth separation of the $R_L$ and $R_T$ responses for low missing momenta as a function of three transfer momenta for $\mathbf{q}$ = 1.0 — 3.0 GeV/c. All measurements will be done in quasi-elastic kinematics. Similar measurements were performed in Hall A on $^3$He, and the proposed measurement on $^4$He will provide information about nuclear density effects. Previous Saclay data [5] taken at $\mathbf{q}$ = 0.3 GeV/c to 0.7 GeV/c note a sizeable quenching of the longitudinal response at $p_m$ = 0.09 GeV/c. Inclusive $^4$He(e,e') data note a quenching of the longitudinal response as well. No such quenching was observed for $^3$He in either inclusive scattering [6] or exclusive scattering [7] measurements. For low missing momenta, the $R_L$ and $R_T$ responses should behave more like those of the proton as the transfered momentum is increased. We hope to observe the transition from a quenched longitudinal response to the predicted value with increased transfered momentum.

Finally in parallel kinematics, we would like to separate the $R_L$ and $R_T$ responses at $p_m$ = 0.300 GeV/c at $\mathbf{q}$ = 1.0 GeV/c in both parallel and anti-parallel kinematics. In this kinematics we will make use of the large energy acceptance of the spectrometers to measure both the two-body-breakup and continuum. The parallel kinematics are in *dip* kinematics where MEC and isobar currents are expected to be large. The anti-parallel measurements have $x_B > 1$, where the above two-body currents as well as FSI are expected to be small while short-range correlations are predicted to be observed.

## 2 Kinematics

The kinematics for the (e,e'p) reaction are shown in Fig. 1. The scattering plane is defined by the incoming electron, $e = (E_e, \mathbf{e})$, and the outgoing electron, $e' = (E'_e, \mathbf{e}')$. The four-momentum of the virtual photon is given by q=(w, $\mathbf{q}$) and the four-momentum of the outgoing proton is given by $p' = (E_p, \mathbf{p}')$. The four-momentum square, $Q^2 = q^2 - \omega^2$, is defined such that for electron scattering $Q^2$ is always positive. The missing momentum vector is defined as $\mathbf{p}_m = \mathbf{q} - \mathbf{p}'$.

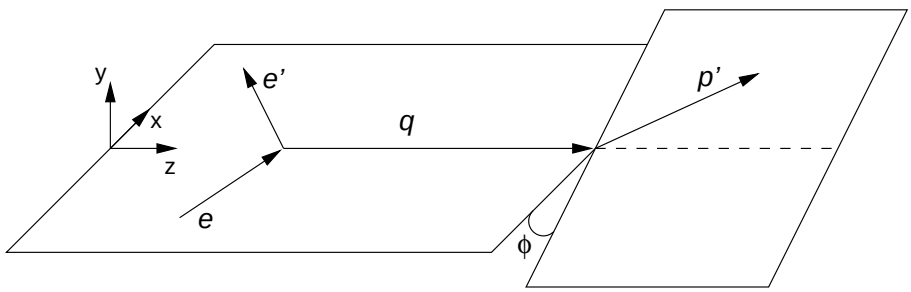


Fig. 1. A schematic of the kinematics for the (e,e'p) reaction.

The form of the differential cross for (e,e'p) reactions in the one-photon exchange approximation for without polarization is:

$$\frac{d^6\sigma}{d\Omega_{e'}dE_{e'}d\Omega_{p'}dE_{p'}} = \frac{E_p p_p}{(2\pi)^3}\sigma_{Mott}\left[v_T R_T + v_L R_L + v_{TL} R_{TL}\cos\phi + v_{TT} R_{TT}\cos 2\phi\right], \quad (1)$$

$$(2)$$

with $\phi$ the angle between the plane defined by $\mathbf{e}$ and $\mathbf{e}'$ and the plane defined by $\mathbf{p}'$ and $\mathbf{q}$, $\sigma_M$ is the Mott cross section,

$$\sigma_{Mott} = \frac{4\alpha^2 E_{e'}^2}{Q^4}\cos^2\frac{\theta_{e'}}{2}. \quad (3)$$

The kinematics factors $v_L, v_T, v_{TL}$,and $v_{TT}$ are:

$$v_L = \frac{Q^4}{\mathbf{q}^4}, \quad (4)$$

$$v_T = \frac{Q^2}{2\mathbf{q}^2} + \tan^2(\theta_e/2), \quad (5)$$

$$v_{TL} = \frac{Q^2}{\mathbf{q}^2}\left[\frac{Q^2}{\mathbf{q}^2} + \tan^2(\theta_e/2)\right]^{1/2}, and \quad (6)$$

$$v_{TT} = \frac{Q^2}{2\mathbf{q}^2}. \quad (7)$$

$$(8)$$

For the two body break-up channel, $^4$He(e,e'p)$^3$H, the proton energy and angle with respect to $\mathbf{q}$ are correlated because the missing energy is fixed. In this case the differential cross is written as follows:

$$\frac{d^5\sigma}{d\Omega_{e'}d\Omega_{p'}dE_{e'}} = \frac{E_p P_p}{(2\pi)^3}\sigma_{Mott} f_{rec}^{-1}\left[v_T R_T + v_L R_L + v_{TL} R_{TL}\cos\phi + v_{TT} R_{TT}\cos 2\phi\right], \tag{9}$$

where $f_{rec}$ is the recoil factor,

$$f_{rec} = \left[1 - \frac{E_{p'}}{E_t}\frac{\mathbf{p_m}\cdot\mathbf{p'}}{p'^2}\right]. \tag{10}$$

The response functions, $R_L, R_T, R_{TL}, R_{TT}$ can be separated by a suitable choice of the kinematic parameters. In perpendicular in-plane kinematics, i.e. constant $\mathbf{q}$ and $\omega$ kinematics, one can separate $R_T$, $R_{TL}$, and a combination of the $R_L$ and $R_{TT}$ response functions, denoted in this proposal as $R_{L+TT}$. One can also measure the cross section asymmetry $A_{TL}$ for a given $\mathbf{q}$ and $\omega$. This asymmetry is defined as:

$$A_{TL} = \frac{\sigma(\phi = 0) - \sigma(\phi = 180)}{\sigma(\phi = 0) + \sigma(\phi = 180)}. \tag{11}$$

In parallel and anti-parallel kinematics, i.e. when the out-going proton is in the direction of $\mathbf{q}$, one can separate the $R_L$ and $R_T$ response functions. In parallel kinematics $p_m$ points in the opposite direction as $\mathbf{q}$ with $x_B < 1$ while in anti-parallel kinematics $p_m$ points in the same direction as $\mathbf{q}$ with $x_B > 1$ where

$$x_B = \frac{Q^2}{2M\omega}, \tag{12}$$

is the Bjorken scaling variable. For $x_B > 1$, the region in $\omega$ between the quasi-elastic peak and the elastic peak is being probed; while for $x_B < 1$, the region $\omega$ towards the delta peak is being probed. The region in $\omega$ between the quasi-elastic peak and delta peak is often referred to as the dip region.

## 3 Physics Motivation

At present, there is a lot of activity in the field of electron scattering from nuclei at a few GeV, aimed at understanding the short range structure of nuclei. It would be ideal to perform theoretical calculations of these processes in a completely microscopic fashion, starting from a Lagrangian. Such an approach would contain explicit relativistic treatments of the nuclear dynamics and the electromagnetic current, as well as a consistent treatment of the initial nuclear state and the in general quite complicated hadronic final state. In practice, for high-energy inelastic electron scattering, it is very difficult to calculate both the nuclear ground state and the final hadronic scattering state consistently in a fully microscopic, relativistic manner. Currently, there are several approximate calculations for particular electro-nuclear reactions available for few-body systems [8,9]. However, it is difficult to extend these approaches for the few-body systems to energies above the pion emission threshold. Considerable effort is being put into this field. We expect that in the next few years calculations for the few GeV regime for reactions with deuteron targets will hopefully become available. Non-relativistic microscopic calculations are available for reactions with $^3$He and $^4$He, which are suitable for reactions at lower energies. However, even the exact, Fadeev-based calculations [10] for $^3$He, lack in their treatment of two-body (MEC and IC) currents. For $^4$He, variational Monte Carlo calculations have been employed [11,12] as well as non-relativistic and relativistic mean-field calculations [13]. Recently, calculations of reactions on few-body systems using Lorentz-integral transform method have been developed [14] and compared to data with relative success. For heavier nuclei, there are only mean-field calculations available, both non-relativistic and lately relativistic as well [13].

In the past years, with the advent of high duty cycle machines with several GeV of beam energy, coincidence experiments with GeV energy and three-momentum transfers have become feasible and are carried out mainly at Jefferson Lab. These high energy and momentum transfers might permit us to study the transition from hadronic degrees of freedom to quark-gluon ( or quark and flux tube ) degrees of freedom in the nucleus. The general philosophy is that if we can not describe a data set with the best "conventional nuclear physics" calculation, involving just hadronic degrees of freedom such as one-body currents and meson exchange currents, isobars, initial and final state correlations, we would see evidence for genuine quark effects in the nucleus. The main practical problem for the time being is that for the realm of several GeV, where the chance to see quark effects is expected to be highest, the "conventional nuclear physics" calculations have not yet been fully developed. Naturally, the interpretation of the data and the extraction of the desired information is feasible only with a detailed knowledge of the whole reaction. Experimental data on few-body systems can serve an extremely useful means of testing any calculations which are being developed. It is very important to obtain as large and as precise as possible a data set, since this is the only effective way to constrain the theoretical models.

### *3.1 Importance of $^4$He*

$^4$He is an essential element in developing "conventional nuclear physics" calculations. It is the simplest nuclear system in which all the basic ingredients of a complex nuclei exist. Its binding energy is similar to that of heavier nuclei and it is reasonable to expect that the behavior of nucleon pairs within this nucleus is similar to that inside heavier nuclei. It is a tightly bound system with strong correlations, providing a better environment for the study of short range effects and nucleon-nucleon correlations in nuclei. Moreover, its study provides an important connection between two- and three-body systems, where exact calculations are possible in both initial and final states of the (e,e'p) reaction, and heavier nuclei where microscopic many body calculations still remain intractable.

$^4$He is small enough for the use of variational Monte Carlo techniques, yet large and dense enough to be treated in the framework of mean field. Each approach has different advantages, with one providing a more microscopic insight, and the other in the use of phenomenology and relativity. Indeed,both approaches have been employed successfully to describe electromagnetic reactions at transfered momenta up to a few hundreds MeV/c, where a large data set is available. A similarly large data set for $^4$He is needed in the few GeV/c regime to facilitate the development of theoretical tools to describe the structure and dynamics which can now be probed. In this respect, studies of both $^3$He and $^4$He are needed to evaluate the effects of the transition from 3 to 4 nucleons, and from a less to a much more dense nucleus. Indeed, existing data indicate a significant difference between the two isotopes. For example, in inclusive (e,e') quasi-elastic scattering, the longitudinal and transverse spectral functions in $^3$He were observed to be the same, whereas in $^4$He the transverse spectral function was larger by 30-40% and in exclusive $^4$He(e,e'p)$^3$H measurements at Saclay a quenching of the longitudinal response by about 35-40% was observed while no such quenching of the longitudinal response was observed for $^3$He(e,e'p)$^2$H. Theoretically, the comparison between $^3$He and $^4$He provides a tool for understanding the inter-relations between microscopic approaches and those of mean field. The proposed measurement on $^4$He will provide data in similar kinematics to recently obtained data in Hall A on $^3$He.

### *3.2 Response Function Separations*

Since describing nuclear reactions in general and electrodisintegration in particular requires understanding of the initial bound state, the currents involved, and the hadronic final state, it is not sufficient to measure only cross sections. Theoretical models have various "knobs" to play with, so a good description of the experimental data can be obtained by introducing various ingredients, with no good way to distinguish between success due to these ingredients. As an example, Fig. 2 presents data by van Leeuwe *et al.* [2] in which a minimum in the cross section at missing momentum around 450 MeV/c which is predicted by factorized calculations is not observed. This predicted "dip" in the cross is due

to the suppression of the s-state wave function in $^4$He at short distances. Calculations are able to fill this minimum by introducing FSI, two-body, and three-body MEC but there is no way to judge the real importance of the various ingredients.

Better understanding of the importance of the various ingredients which go into the theoretical models can be obtained by measuring as many as possible independent observables. This has traditionally been done mainly by varying the kinematics in a way which enhance or suppress specific ingredients. A unique tool in this respect is the separation of response functions and asymmetries each of which, in general, is sensitive to a different ingredient in the calculations. We illustrate this point by two recent examples. In the data of J. Gao *et al.* [3] the importance of dynamical relativistic effects was clearly demonstrated by a unique structure in the $A_{TL}$ asymmetry which is predicted by calculations only if these effects are properly included. In the new Bates data on the electrodisintegration of the deuteron, their comparison to calculations by Arenhovel and Tjon [15] demonstrates that by measuring $R_{TL}$, $R_{TT}$ and $R_{TL'}$, it is possible to understand the data in terms of proper inclusion of FSI, MEC, IC, and relativistic effects [15].

### *3.3 Overview of Existing Data*

*The following review of existing data is by no means exhaustive. However, it describes all data which are relevant to this proposal.*

The most complete $^4$He(e,e'p)$^3$H cross section measurement to date was performed at NIKHEF by van Leeuwe *et al.* [1,2]. The cross section was measured in the dip region with $x_B = 0.29$ at $Q^2 = 0.0115$ GeV/c and with a virtual-photon polarization of 0.63. Using perpendicular kinematics, the cross section was measured for missing momentum in the range of 220-690 MeV/c, as seen in Fig. 2. The measured cross sections for $p_m < 300$ MeV/c agree well with PWIA calculations by Laget [16], Schiavilla [12] and Nagorny [17,18], While for $p_m > 600$ MeV/c, the measured cross sections agree with these authors' calculations which include different prescriptions for treating FSI, MEC or tree-type and one-loop diagrams. Only Nagorny's calculations describe the data reasonably well for $400 < p_m < 500$ MeV/c.

More recently, Jefferson Lab experiment E97-111 [4] completed measurements of the $^4$He(e,e'p)$^3$H cross section for missing momenta up to 500 MeV/c in both perpendicular and parallel kinematics. Motivated by the NIKHEF experiment, this experiment searched for the predicted minimum around $p_m = 425$ MeV/c with the assumption that parallel kinematics measurements are less sensitive to final-state interactions, which were presumed to fill the minimum in the NIKHEF experiment. The data are still under analysis; however, preliminary results indicate that the predicted minimum is not observed.

Response functions were extracted for the $^4$He(e,e'p)$^3$H reaction in several experiments. The interference $R_{TL}$ response was measured at Bates [19] in dip kinematics with ( $x_B = 0.24$ ) at $Q^2 = 0.09$ GeV/c. The data were best described by calculations by Schiavilla [12]

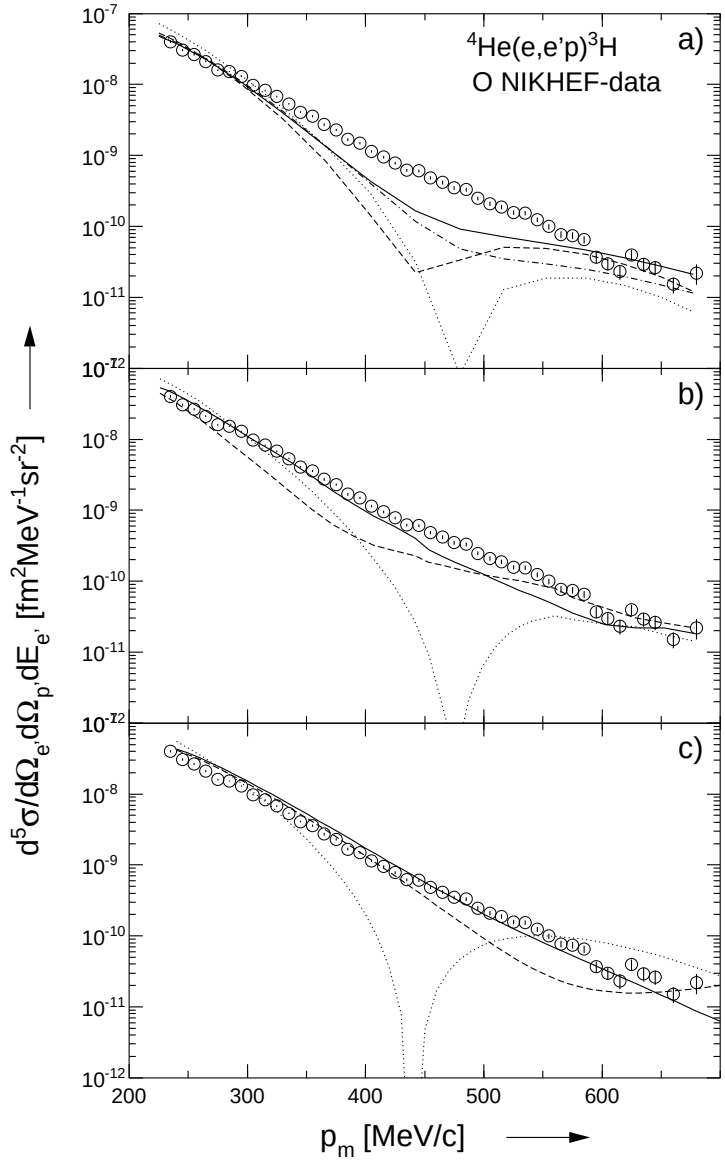


Fig. 2. Shown above is results from van Leeuwe *et al* [2]. The fivefold differential $^4$He(e,e'p)$^3$H cross section as a function of the missing momentum for $\omega = 215$ MeV and $\mathbf{q} = 401$ MeV/c. The calculations in the top figure were performed by J.-M. Laget [16]. The dotted curve is the PWIA calculation, the dashed includes FSI, the dot-dashed includes two body MEC, and the solid includes three-body MEC. The calculations for the middle figure were performed by R. Schiavilla [11]. The dotted curve is the PWIA calculation, the dashed curve includes FSI, and the solid curve includes two-body currents. The calculations for the bottom figure were performed by S. Nagorny [17,18]. The dotted curve is the PWIA calculation, the dashed includes tree-type diagrams, and the solid includes one-loop diagrams.

which include correlated wave function for the proton-triton scattering state. MEC are required for better agreement with the data. The longitudinal and transverse responses were extracted by Rosenbluth separation in quasi-elastic kinematics at Saclay [5]. The measurements were done at $p_m = 30$, 90, and 190 MeV/c for a range of transfered momenta $\mathbf{q} = 0.3$ - 0.83 (GeV/c)$^2$. All measurements were done in parallel kinematics. Comparison of the data to the calculations of Schiavilla [11] and Laget [20] resulted in the conclusion that the longitudinal response is quenched by up to 35-40% upto the highest $p_m$ and $\mathbf{q}$. The authors further claim that this quenching may be an indication of the modification of the nucleon form factors in the nuclear medium. No such quenching was observed for the transverse response, nor for either the longitudinal or transverse responses in $^3$He(e,e'p)$^3$H and $^2$H(e,e'p)n [5].

Recent measurements at Mainz were performed with a fixed transfered momentum $\mathbf{q} =$ 686 MeV/c. The measurements by R. Florizone *et al.* [21] was performed in quasi-elastic kinematics ($\omega = 243$ MeV) while the measurements by A. Kozlov *et al.* [22,23] were performed in dip kinematics ($\omega = 334$ MeV). The cross sections were measured for three electron kinematics (three virtual-photon polarizations) in both experiments. Although no Rosenbluth separation was reported for Florizone's data, the author deduced the longitudinal/transverse behavior of the cross-sections, by removing their dependence on the off-shell electron-proton cross section, $\sigma_{CC1}$ as prescribed by de Forest [24]. He concluded, that in quasi-elastic $^4$He(e,e'p)$^3$H reaction, the longitudinal/transverse behavior of the cross section for missing momenta up to at least 90 MeV/c, is completely determined by $\sigma_{CC1}$, in disagreement with the conclusion of Ducret [5]. Not surprisingly, the data in the dip region by Kozlov does show a larger transverse than longitudinal spectral function by approximately 30 percent.

There exist also several data sets for the semi-inclusive $^4$He(e,e'p)pnn reaction, all at transfered momenta of a few hundreds MeV/c. For example, J.J. van Leeuwe *et al.* [1,25] measured the cross sections in dip kinematics ($x_B$=0.29) for at $Q^2 = 0.115$ (GeV/c)$^2$ at NIKHEF. The data are for missing energies up to 120 MeV, and missing momenta up to 600 MeV/c. They observe a large enhancement of the cross sections at high missing energies at increasing missing momenta. Comparing the data to calculations by Laget, the authors attribute this enhancement to two-body MEC and IC currents, as well as to short-range correlations which were explicitly included in Laget's wave function. Similar enhancement of the cross section at large missing energies for increasing missing momenta was observed by N. Liyanage *et al.* [26] in recent $^{16}$O(e,e'p) data from Jefferson Lab at much higher momentum transfer, $Q^2 = 0.8$ (GeV/c)$^2$, for which calculations by Ryckebysch *et al.* [27] arrive at a similar conclusion.

Data from Saclay [28] in kinematics $0.4 < x_B < 1.8$ also note a peak in the missing energy spectra for various missing momenta, as shown in Fig. 3. In addition to becoming more pronounced as the missing momentum increases, the peak moves to higher missing energies with increased missing momenta. The location of the peak corresponds to the

expected location of the correlated two-nucleon peak given by,

$$E_m = E_{thr} + \left(\frac{A-2}{A-1}\right)\frac{p_m^2}{2m_p} \tag{13}$$

where $E_{thr}$ is the missing energy corresponding to the continuum threshold, $p_m$ is the missing momentum, and $m_p$ is the mass of the proton.

In MAMI, both Florizone [21] and Kozlov [22] measured the cross sections at high missing energies. They also studied the longitudinal/transverse behavior by integrating the cross-section over the measured range of missing momenta. In Florizone's quasi-elastic kinematics, the L/T behavior follows that of $\sigma_{CC1}$, while at Kozlov's dip kinematics the transverse spectral function is increasingly larger than the longitudinal for increasing missing energies. Both data sets were compared to calculations by Efros *et al.* [14] which employ Lorentz integral transform method. For both missing energy spectra and continuum "distorted" momentum distributions the calculations agree reasonably well with both data sets, perhaps better with the quasi-elastic data of Florizone.

It is useful here to mention the recently completed experiment in Hall A on $^3$He [29]. In this experiment, the $^3$He(e,e'p) cross sections and response functions were measured for large transfer momenta. A detailed description of these measurements is given in Section 4.1. The data are under analysis and preliminary results are already emerging. It is clear that the data are of very high quality and the challenge of response function separation at these kinematics can be met. It is important to note that our proposed measurement on $^4$He will provide cross section and separated response functions in similar kinematics to those of the $^3$He measurement. These data, in addition to their inherent value, will facilitate a very meaningful comparison between $^3$He and $^4$He in similar kinematics.

### *3.4 Motivation for Perpendicular Kinematics*

The perpendicular kinematics is suitable for measuring the cross sections up to very high missing momentum and is needed for the separation of the longitudinal-transverse interference response, $R_{TL}$, and asymmetry $A_{TL}$. It is also possible to separate the transverse response $R_T$ and a combination of the longitudinal and transverse-transverse interference responses $R_{L+TT}$. All variables can be measured in the same transfered momentum $\mathbf{q}$ and energy $\omega$, hence fixed kinematic conditions.

The Jefferson Lab PAC has already approved with high priority a measurement of the $^{16}$O(e,e'p) reaction to the valence 1p states [30] whose purpose is to test the limit of the single-particle model by measuring the cross sections, $R_{TL}$ and $A_{TL}$ to high missing momenta. While in the case of $^{16}$O only mean-field calculations, albeit relativistic, are available, $^4$He provides tests for both relativistic mean field and microscopic calculations with each having its own advantages and limitations. At a fixed quasi-elastic electron

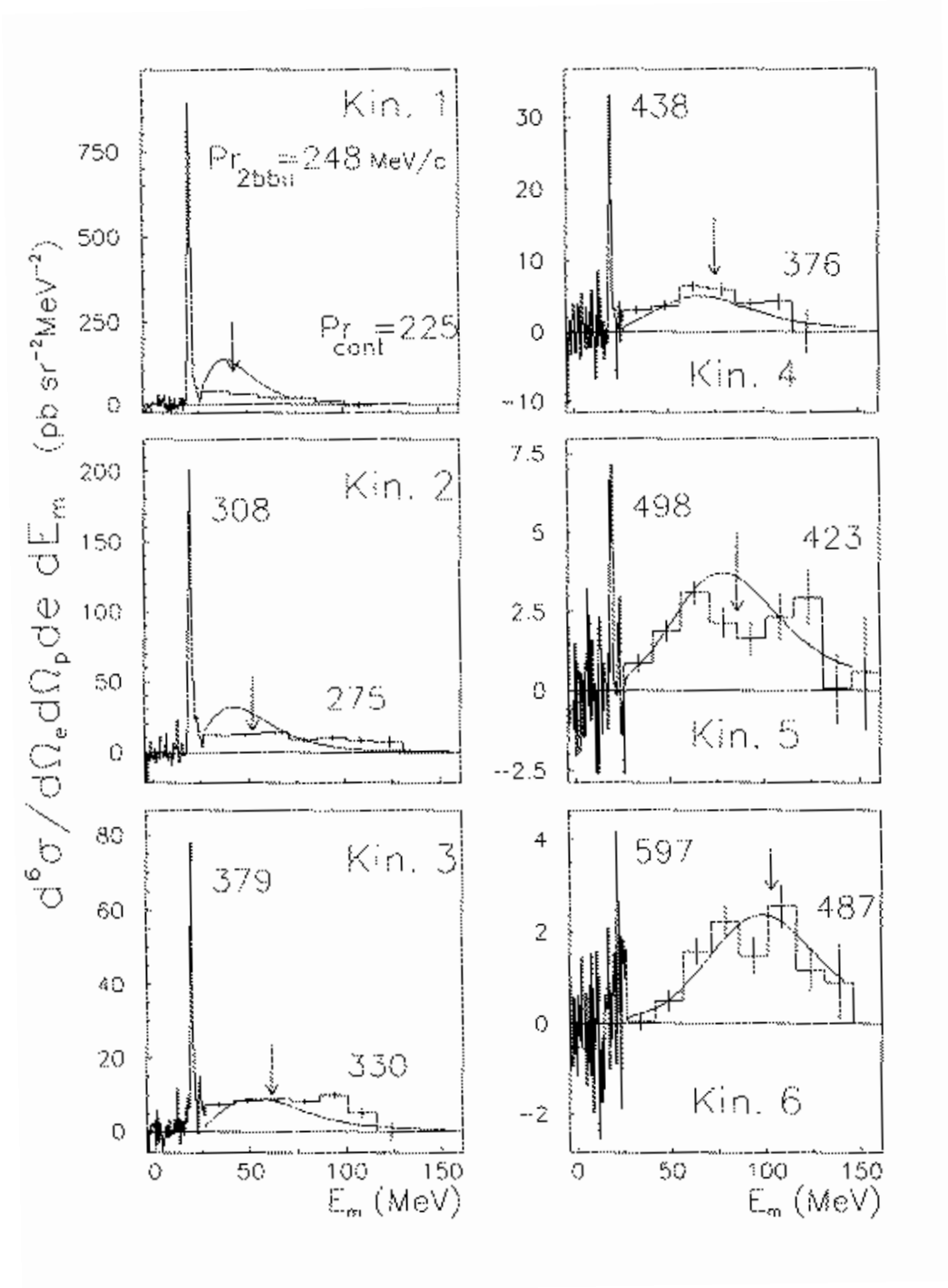


Fig. 3. Shown above the data from J.M. Le Goff *et al.* [28]. The radiatively corrected experimental cross section for various kinematics are shown as a function of missing energy, $p_m$. The arrow indicates where the nucleon-nucleon peak is expected. The curves are the result of a microscopic calculation by J.-M. Laget.

kinematics with transfered momentum q = 1.5 GeV/c we intend to measure the cross section for missing momenta up to 1.2 GeV/c, and $R_{TL}$ and $A_{TL}$ up to $p_m = 0.50$ GeV/c. These measurements will not only extend substantially the range of missing momenta, but will also provide a complete data set in the same kinematics conditions. At this high transfered momentum, we expect that FSI can be treated successfully in the Eikonal approximation. Yet, the comparison to relativistic mean-field calculations that employ optical potentials, which were very successful in describing J. Gao's recent Hall A data [3] on $^{16}$O, is also very valuable.

The quasi-elastic kinematics facilitates the comparison of the data to single-particle models for the lower range of the missing momentum, providing a "benchmark" set of data to the theoretical models. At high missing momenta, we expect the single-particle models to break down and so each model will have to resort to its unique ingredients for describing the data. The availability of $R_{TL}$ and $A_{TL}$ in addition to the cross sections will significantly constrain these ingredients. These ingredients will be constrained even further by the comparison to the data already available in similar kinematics from the recently completed experiment on $^3$He. For missing momentum $p_m$ between 0.325 GeV to 0.575 GeV, we propose to measure the cross section at a second electron angle but at the same transfered momentum and energy. This will allow the extraction of $R_T$ and $R_{L+TT}$ as well for this range of missing momenta. We note that most models predict a minimum in the proton-triton momentum distribution at $p_m = 425$ MeV/c, which has not been observed for low or high transfered momenta or in either perpendicular or parallel kinematics [2,4]. This minimum can be filled by the breakup of the factorization in many calculations due to FSI, MEC, IC, or dynamical relativistic effects. The availability of the cross section, $R_{TL}$, $A_{TL}$, $R_T$ and $R_{L+TT}$ for this $p_m$ range will greatly constrain the ingredients that are used to break the factorization.

### *3.5 Motivation for Parallel Kinematics*

We propose to extract the longitudinal and transverse response functions for several transfered momenta, $\mathbf{q}$ = 1, 1.5, 2, 3 GeV/c, by performing Rosenbluth separation in quasi-elastic parallel kinematics. The measurements will be done for low missing momenta. Ducret *et al.* [5] observed a quenched longitudinal response at $Q^2 < 0.6$ (GeV/c)$^2$, which they attributed to modification of the nucleon form factor in the dense $^4$He medium. It will be very interesting to investigate the evolution of this effect with momentum transfer. Again, the high transfered momentum allows the use of the Eikonal approximation for treatment of the final-state interactions and the use of parallel kinematic will also help in minimizing the effects of FSI. The data will be compared to similar data recently obtained for $^3$He in the same kinematics [29], allowing for a unique study of density effects. We note that these measurements are proposed where the cross sections are very high, and the beam-time required is small, providing a very favorable cost-benefit balance for this measurement.

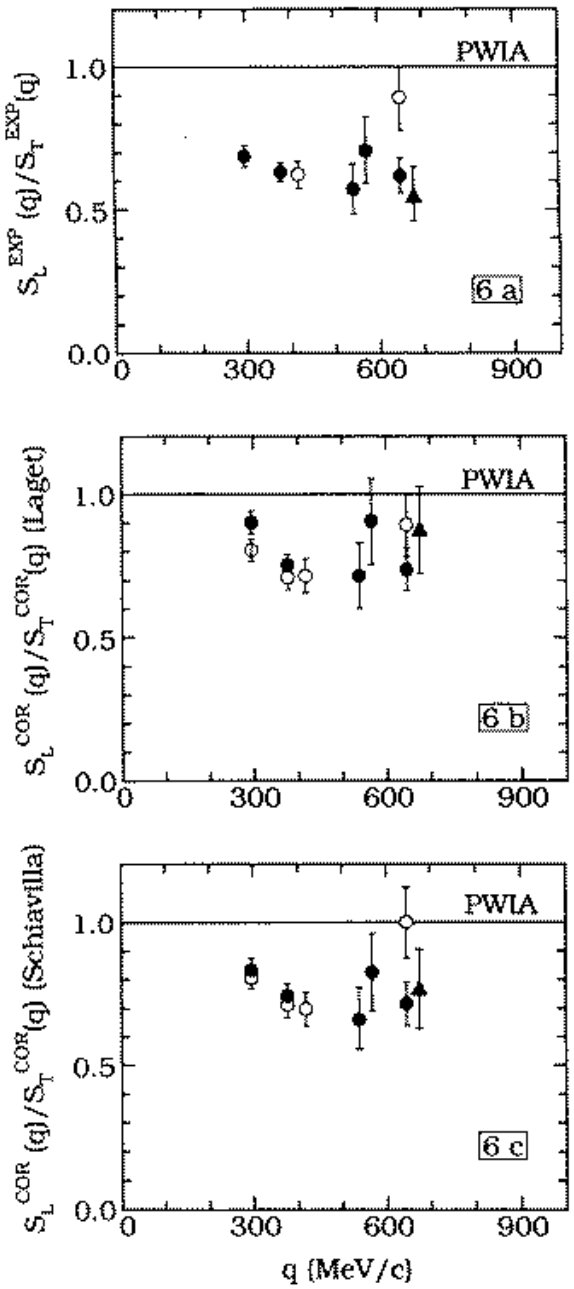


Fig. 4. The data of Ducret *et al* [5]. The ratio of longitudinal to transverse spectral functions as a function of momentum transfer **q**. Open circles correspond to $p_m = 30$ MeV/c, the solid circles correspond to $p_m = 90$ MeV/c, and the solid triangles correspond to $p_m = 190$ MeV/c. The horizontal lines indicate the PWIA ratio. In upper most plot, the experimental spectral functions $S_L^{EXP}/S_T^{EXP}$ is shown, in the middle plot the ratio of the spectral functions is shown with correction factors from J.-M. Laget [20], and in the bottom figure the ratio of the spectral functions is shown with correction factors from R. Schiavilla [12].

We propose also to extract the longitudinal and transverse response functions in two non-quasielastic parallel kinematics. The $R_L$ and $R_T$ responses will be measured for the same missing momentum, $p_m = 0.3$ GeV/c, in parallel and anti-parallel kinematics for the reaction $^4$He(e,e'p)X. The measurement will be done for transfered momenta of 1 GeV/c. Again, with this high transfered momentum, and especially for parallel and antiparallel kinematics, we expect the FSI to be under theoretical control. For the parallel kinematics, $x_B < 1$, measurement, we expect an enhanced transverse response due to MEC and IC, while for antiparallel kinematics, $x_B > 1$, we expect these two-body currents to be insignificant while short-range nucleon-nucleon correlations are predicted to be observed.

## 4 Relation to other Jefferson Lab Proposals

### *4.1 Hall A Experiment 89-044*

The aim of this experimental program was to investigate three specific aspects of the electromagnetic response of $^3$He through (e,e'p) coincidence measurements. In perpendicular kinematics, with a constant $\mathbf{q}$ = 1.5 GeV/c and $\omega$ = 0.845 GeV, the single nucleon structure of $^3$He was studied with special emphasis on high momenta, up to 1 GeV/c in missing momentum. We also did a complete in-plane separation of the response functions $R_{TL}$, $R_T$, and the combination of $R_{L+TT}$ up to missing momenta of 0.55 GeV/c. In parallel kinematics, the $\mathbf{q}$ dependence of the reaction was determined by performing an $R_L/R_T$ (longitudinal/transverse) Rosenbluth separation for protons emitted along $\mathbf{q}$ (in parallel kinematics), up to $\mathbf{q}$ = 3 GeV/c. This was performed in both quasifree kinematics ($p_m$ = 0) and for q = 1 and 2 GeV/c at $p_m \pm 0.3$ GeV/c. Also, the continuum region was studied in order to search for correlated nucleon pairs. This was done in both parallel and perpendicular kinematics with full in-plane separation of the response functions.

For the present proposal on $^4$He we have decided to use the same kinematic conditions, $\mathbf{q}$ = 1.5 GeV/c and $\omega$ = 0.84 GeV, as was used for the $^3$He experiment. Based on discussions with R. Schiavilla and S. Jeschonnek, this choice of kinematics will facilitate a comparison of the results from $^4$He and $^3$He.

### *4.2 Hall A Experiment 97-111*

Data collection for this approved experiment was completed in Fall, 2000. The aim of this proposal was to measure cross sections for the $^4$He(e,e'p)$^3$H reaction in a range of missing momenta which spanned the theoretically predicted minimum at $p_m$ = 0.425 GeV/c. The depth of the minimum in the cross section reflects the minimum in the spectral function for the triton ground state transition. The minimum is expected to be clearly seen if the Plane Wave Impulse Approximation is valid. Meson exchange currents and final state interactions tend to fill the minimum in the cross section. E97-111 was performed for two settings of constant q-$\omega$ which gave a kinetic energy of the proton in the triton's rest frame of 0.345 GeV. In the proposed experiment for perpendicular kinematics we will maintain a kinetic energy of the proton in the triton's rest frame of 0.809 GeV. At this higher energy the final state interactions can be treated using either the generalized Glauber approximation, or by an optical potential. E97-111 also measured in parallel kinematics for the positive y configuration ( $\cos(\theta_{qx}) = -1$.) in two settings. The proton's kinetic energy in the triton's rest frame varied from 0.77 GeV to 1.86 GeV in this experiment. Missing momenta to 0.5 GeV/c were investigated. In the proposed experiment for parallel kinematics we will vary the kinetic energy of the proton in the triton's rest frame from 0.433 to 2.205 GeV for the $\mathbf{q}$ survey from 1 to 3 GeV/c, and we will do a longitudinal/transverse

separation at $p_m = 0.30$ GeV/c. No separations in response functions were attempted in E97-111, whereas this is a goal of the current proposal.

### *4.3 Hall A Experiment 97-011*

This experiment was originally approved but was taken off the books after the jeopardy period. The aim of this experiment was to study high momentum components in $^3$He and $^4$He measuring both the two body and multi particle breakup at $Q^2 = 2$ and 3 (GeV/c)$^2$ and $x_B > 1$. Absorption of a virtual photon by a nucleon of a correlated pair, is expected to produce a distinctive ridge in the missing energy vs. missing momentum plane. The existence of this ridge in data taken earlier at Saclay for $^4$He(e,e'p)pnn was taken as evidence for nucleon-nucleon correlations. If this ridge is at high missing momentum, then the correlations are associated with a short-range interaction. Cross sections in anti-parallel kinematics were to be measured for both nuclei at y = -0.3 and -0.45 GeV/c ($x_B$ = 1.51 and 1.80 respectively for $^4$He). The kinematics were chosen so that meson exchange and isobar currents as well as final state interactions should be minimized. We intend to measure both the parallel and antiparallal $p_m = 0.3$ GeV/c cross sections and $R_L/R_T$ response functions as part of this proposal.

### *4.4 Hall B Experiment 89-027/91-009*

Measurements were made using the CLAS on $^3$He, $^4$He, $^1$2C and $^5$6Fe with 1.1, 2.2 and 4.4 GeV electrons in 1999 with polarized beam [31,32] (Measurements were not made on $^4$He at 1.1 GeV.) Good $R_{TL'}$ separations were obtained and the experimenters are also looking into possible $R_{TL}$ separations. $R_L/R_T$ separations are impossible at this time (and probably always). This measurement's energy resolution is about 20 MeV (at 2.2 GeV), making it rather difficult to resolve discrete states (i.e. cleanly resolve the proton-triton channel from the three-body breakup channel in $^4$He(e,e'p)X. In order to obtain an estimate of the ground state counts they need to extrapolate the tails of other reaction that go into this low $E_m$ region. For example, integrating the spectrum out to a missing energy of about 130 MeV, summing over all allowed Q$^2$ for 0.8 $GeV < \omega < 1.1$ $GeV$ they have been able to obtain $R_{TL'}$ to about 400 - 500 MeV/c in missing momentum.

There is no real overlap between these data and our proposed measurement. The CLAS experiment covers a far greater kinematic range (in Q$^2$ and $\omega$) than this Hall A proposal, can measure the out-of-plane response functions in some kinematics and can measure 2 (or more) nucleon knockout. In order to do this, they need to integrate over a significantly larger Q$^2$ and $\omega$ bin than we will measure. The CLAS is very well suited for surveys of the dominant reaction channels. However, for detailed studies of specific reaction channels in extreme kinematical conditions, the high luminosity, high resolution Hall A spectrometers are the most optimal choice.

## 5 Experimental Setup

Hall A has proven itself capable of extracting high quality response function [3,26]. In fact, these results from the reaction $^{16}$O(e,e'p) came from the first experiment to be performed in Hall A and since then the knowledge of the spectrometers has been continually improving. Presently, the analysis of the $^{3}$He(e,e'p) experiment is underway and there is an approved Hall A experiment to measure accurate cross sections and extract the response functions from the $^{2}$H(e,e'p) reaction.

We plan to measure the reaction (e,e'p) in $^{4}$He, by making use of the techniques developed from these experiments, the Hall A high resolution spectrometers, and the cryogenic high pressure $^{4}$He target. With a missing energy resolution of 1 Mev, the two-body peak, located at 19.8 MeV, will be well separated from the three- and four-body break-up continuum which start at 26.1 MeV and 28.3 MeV respectively.

Cross sections, count rate calculations, and simulations for the proposed measurements were estimated using a beam current of 75 uA on a 10 cm long "tuna can" $^{4}$He cryogenic target with a density of 0.14 g/cm$^{3}$. This translates to a target luminosity of $1 \times 10^{38}$ cm$^{-2}$ sec$^{-1}$. A 20 cm long "beer can" $^{4}$He cryotarget is presently under construction which would essentially double the proposed target luminosity. Since this new target would be narrower, it would have the additional benefit of reducing the multiple scattering of the ejected particles, thus resulting in a better missing energy resolution.

The standard properties of the Hall A spectrometers were used in making the count rate estimates: solid angles of 5 msr and momentum bites of +/- 4.5%. We used a spectral function $S(p_m)$ which we parametrized from existing data on $^{4}$He. In the low $p_m$ region (0-200 MeV/c) we used the spectral function determined from the Mainz [33,21] and NIKHEF [34] data. Above 200 MeV/c we parametrized the spectral function data of van Leeuwe *et al.* [1,2] with an exponential fit. The resulting parameterization of the spectral function is shown in Fig. 5. We believe using this parameterization of the spectral function extracted from experimental data for the determination the $^{4}$He(e,e'p)$^{3}$H cross sections is more realistic than using any determined from the various models. Also shown in the figure is the triton-proton momentum distribution obtained with the recent Argonne V18l [35] wavefunctions normalized to the same value of the integral as the experimental parameterization.

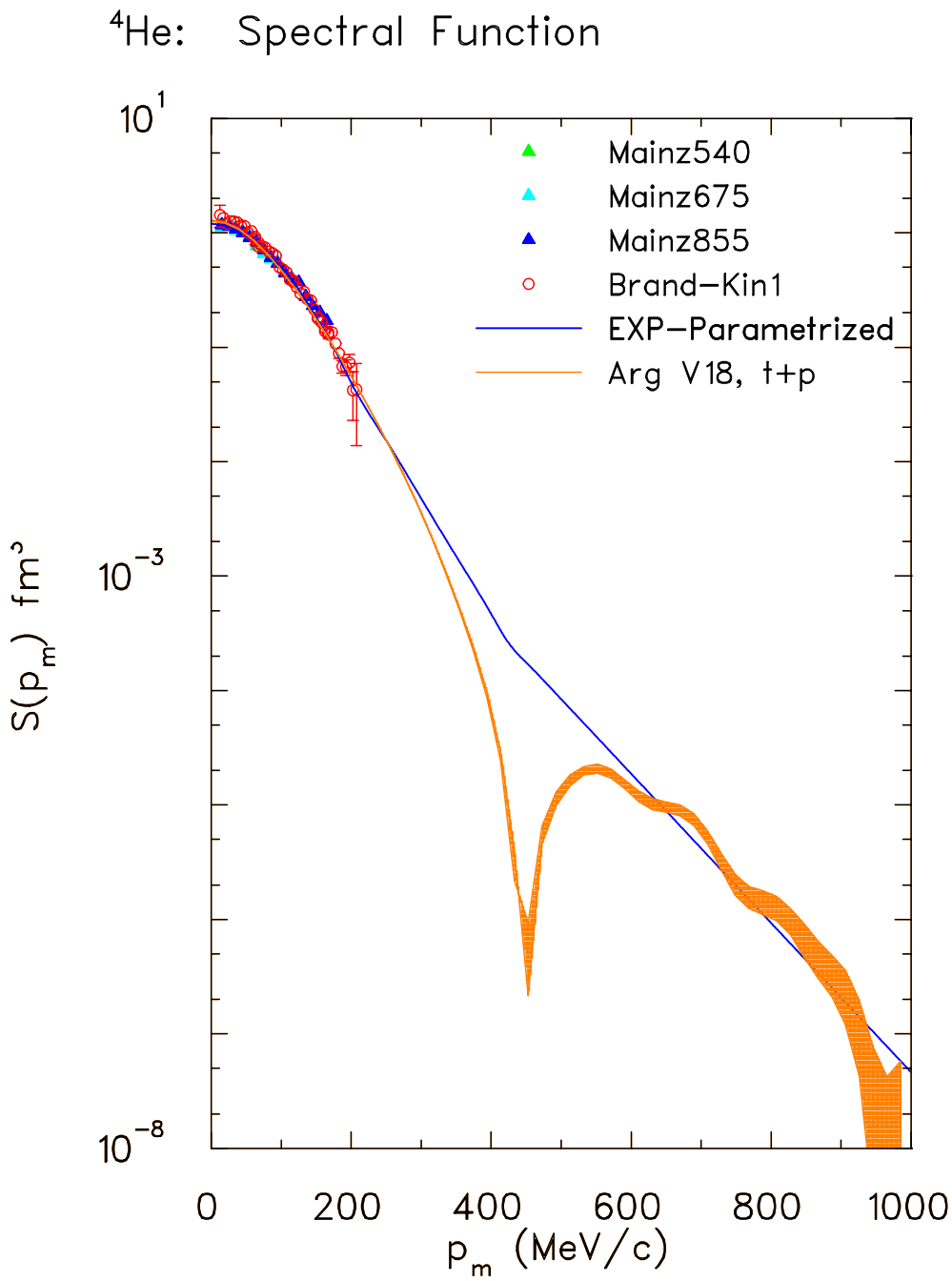


Fig. 5. Shown above is the parameterization of the $^4$He spectral function. Also shown is the momentum distribution obtained from the recent Argonne V18 wavefunctions normalized to the same value of the integral as the experimental parameterization.

### *5.1 Proposed Kinematics*

In the perpendicular kinematics, shown in Table 1, $q$ will be fixed to 1.50 GeV/c and $\omega$ will be fixed to 0.837 GeV. With this constraint, the (e,e'p) cross section will first be measured with a beam energy of 4.80 GeV with proton detected on either side of the q-vector. This will allow the extraction of the $R_{TL}$ response function and the $A_{TL}$ asymmetry. Using a different beam energy, we measure the cross section for a $p_m$ around zero, 0.400, and 0.500 GeV/c at a different epsilon. This will along the extraction of the $R_{L+TT}$ and $R_T$ response functions. The final few kinematics will extend our knowledge of the $^4$He(e,e'p) cross section to a $p_m = 1$ GeV/c.

In Table 2 the high missing momentum kinematics are shown. From the recent Hall A $^3$He(e,e'p)d results, we expect the strength in the cross section as a function of missing momentum to be much higher than presently predicted. We are therefore requesting time to measure to as large a values of $p_m$ as possible.

In parallel kinematics, shown in Table 3, the detected proton is emitted in the direction defined by the q-vector. With this constraint, the (e,e'p) cross section will be measured for a number of different transfer momenta and with different epsilon values. This will allow the extraction of the $R_L$ and $R_T$ response functions as a function of transfer momentum. These kinematics can be broken into two parts. The first is the low $p_m$ high $\mathbf{q}$ to investigate the quenching of the longitudinal response function. The second is the high $p_m$ points to investigate nucleon-nucleon correlations by making $^4$He(e,e'p)pnn measurements in anti-parallel and parallel kinematics.

### *5.2 Singles Rates*

The single-arm background rates is shown for the perpendicular kinematics in Table 4, for the high missing momentum in Table 5, and for parallel kinematics in table 6. The (e,e') rate were calculated with the QFS computer code and the (e,p),(e,$\pi^+$), and (e,$\pi^-$) rates were calculated with the EPC code of Lightbody and O'Connell [36]. The rates were calculated for a luminosity of $1.0 \times 10^{38}$ cm$^2$/s. As demonstrated during the E89-044 $^3$He(e,e'p) experiment, which made measurements in similar kinematics, rates such as these are not a problem for the Hall A spectrometers.

### *5.3 Coincidence Rates*

We determined the coincidence rates by assuming a luminosity of $1 \times 10^{38}$ cm$^{-2}$ sec$^{-1}$. A missing energy width of 1.6 MeV and a timing width of 2 ns was used to determine the true and accidental rates. The computer code SEEX [37] was used in computing the fivefold differential cross sections (denoted as $\sigma 5$ in the tables) at each kinematic point.

Table 1
Perpendicular Kinematics

| Kinematics | $\mathbf{q}$ [GeV/c] | $E_o$ [GeV] | $\omega$ [GeV] | $\epsilon$ | $E_e$ [GeV] | $\theta_e$ [degrees] | $P_p$ [GeV] | $\theta_p$ [degrees] | $p_m$ [GeV/c] |
|---|---|---|---|---|---|---|---|---|---|
| Kin01 | 1.50 | 4.80 | 0.840 | 0.943 | 3.96 | 16.4 | 1.49 | 48.2 | 0.000 |
| Kin02 | 1.50 | 1.25 | 0.840 | 0.101 | 0.41 | 120. | 1.49 | 13.6 | 0.000 |
| Kin03 | 1.50 | 4.80 | 0.840 | 0.943 | 3.96 | 16.4 | 1.49 | 52.0 | 0.100 |
| Kin04 | 1.50 | 4.80 | 0.840 | 0.943 | 3.96 | 16.4 | 1.49 | 44.4 | 0.100 |
| Kin05 | 1.50 | 4.80 | 0.840 | 0.943 | 3.96 | 16.4 | 1.48 | 55.8 | 0.200 |
| Kin06 | 1.50 | 4.80 | 0.840 | 0.943 | 3.96 | 16.4 | 1.48 | 40.5 | 0.200 |
| Kin07 | 1.50 | 4.80 | 0.840 | 0.943 | 3.96 | 16.4 | 1.47 | 59.7 | 0.300 |
| Kin08 | 1.50 | 4.80 | 0.840 | 0.943 | 3.96 | 16.4 | 1.47 | 36.6 | 0.300 |
| Kin09 | 1.50 | 4.80 | 0.840 | 0.943 | 3.96 | 16.4 | 1.45 | 63.6 | 0.400 |
| Kin10 | 1.50 | 4.80 | 0.840 | 0.943 | 3.96 | 16.4 | 1.45 | 32.7 | 0.400 |
| Kin11 | 1.50 | 1.25 | 0.840 | 0.101 | 0.41 | 120. | 1.45 | 29.1 | 0.400 |
| Kin12 | 1.50 | 4.80 | 0.840 | 0.943 | 3.96 | 16.4 | 1.44 | 67.6 | 0.500 |
| Kin13 | 1.50 | 4.80 | 0.840 | 0.943 | 3.96 | 16.4 | 1.44 | 28.7 | 0.500 |
| Kin14 | 1.50 | 1.25 | 0.840 | 0.101 | 0.41 | 120. | 1.44 | 33.1 | 0.500 |

Table 2
High Missing Momentum Kinematics

| Kinematics | $\mathbf{q}$ [GeV/c] | $E_o$ [GeV] | $\omega$ [GeV] | $\epsilon$ | $E_e$ [GeV] | $\theta_e$ [degrees] | $P_p$ [GeV] | $\theta_p$ [degrees] | $p_m$ [GeV/c] |
|---|---|---|---|---|---|---|---|---|---|
| Kin15 | 1.50 | 4.80 | 0.840 | 0.943 | 3.96 | 16.4 | 1.41 | 71.7 | 0.600 |
| Kin16 | 1.50 | 4.80 | 0.840 | 0.943 | 3.96 | 16.4 | 1.37 | 78.0 | 0.750 |
| Kin17 | 1.50 | 4.80 | 0.840 | 0.943 | 3.96 | 16.4 | 1.32 | 84.7 | 0.900 |
| Kin18 | 1.50 | 4.80 | 0.840 | 0.943 | 3.96 | 16.4 | 1.26 | 91.8 | 1.050 |
| Kin19 | 1.50 | 4.80 | 0.840 | 0.943 | 3.96 | 16.4 | 1.19 | 99.6 | 1.200 |

Table 3
Parallel Kinematics

| Kinematics | $\mathbf{q}$ [GeV/c] | $E_o$ [GeV] | $\omega$ [GeV] | $\epsilon$ | $E_e$ [GeV] | $\theta_e$ [degrees] | $P_p$ [GeV] | $\theta_p$ [degrees] | $p_m$ [GeV/c] |
|---|---|---|---|---|---|---|---|---|---|
| Kin20 | 1.00 | 4.05 | 0.453 | 0.966 | 3.59 | 13.4 | 1.00 | 56.6 | 0.000 |
| Kin21 | 1.00 | 0.845 | 0.453 | 0.210 | 0.392 | 102 | 1.00 | 22.6 | 0.000 |
| Kin22 | 2.00 | 4.80 | 1.29 | 0.890 | 3.51 | 21.5 | 1.94 | 39.9 | 0.000 |
| Kin23 | 2.00 | 1.95 | 1.29 | 0.260 | 0.659 | 84.7 | 1.94 | 19.2 | 0.000 |
| Kin24 | 3.00 | 4.80 | 2.23 | 0.716 | 2.58 | 33.3 | 3.00 | 28.1 | 0.000 |
| Kin25 | 3.00 | 2.90 | 2.23 | 0.174 | 0.675 | 92.0 | 3.00 | 13.0 | 0.000 |
| Kin26 | 1.00 | 4.05 | 0.268 | 0.968 | 3.78 | 14.2 | 0.70 | 67.5 | 0.300 |
| Kin27 | 1.00 | 0.845 | 0.268 | 0.338 | 0.576 | 87.3 | 0.70 | 33.3 | 0.300 |
| Kin28 | 1.00 | 2.90 | 0.701 | 0.926 | 2.20 | 16.2 | 1.30 | 38.0 | -0.300 |
| Kin29 | 1.00 | 1.25 | 0.701 | 0.528 | 0.549 | 51.0 | 1.30 | 25.3 | -0.300 |

Table 4
Singles rates for the perpendicular kinematics.

| Kinematics | (e,e') KHz | (e,$\pi^-$) KHz | (e,p) KHz | (e,$\pi^+$) KHz |
|---|---|---|---|---|
| Kin01 | 12 | 18 | 96 | 25 |
| Kin02 | <1 | <1 | <1 | <1 |
| Kin03 | 12 | 18 | <1 | <1 |
| Kin04 | 12 | 18 | 13 | 26 |
| Kin05 | 12 | 18 | <1 | <1 |
| Kin06 | 12 | 18 | 135 | 26 |
| Kin07 | 12 | 18 | <1 | <1 |
| Kin08 | 12 | 18 | 150 | 27 |
| Kin09 | 12 | 18 | <1 | <1 |
| Kin10 | 12 | 18 | 160 | 27 |
| Kin11 | <1 | <1 | 5. | <1 |
| Kin12 | 12 | 18 | <1 | <1 |
| Kin13 | 12 | 18 | 200 | 28 |
| Kin14 | <1 | <1 | 3. | <1 |

Table 5
Singles rates for the high missing momentum.

| Kinematics | (e,e') KHz | (e,$\pi^-$) KHz | (e,p) KHz | (e,$\pi^+$) KHz |
|---|---|---|---|---|
| Kin15 | 12 | 18 | <1 | <1 |
| Kin16 | 12 | 18 | <1 | <1 |
| Kin17 | 12 | 18 | <1 | <1 |
| Kin18 | 12 | 18 | <1 | <1 |
| Kin19 | 12 | 18 | <1 | <1 |

Table 6
Singles rates for the parallel kinematics.

| Kinematics | (e,e') KHz | (e,$\pi^-$) KHz | (e,p) KHz | (e,$\pi^+$) KHz |
|---|---|---|---|---|
| Kin20 | 165 | 19 | 98 | 21 |
| Kin21 | <1 | <1 | 206 | <1 |
| Kin22 | 1.4 | 23 | 100 | 27 |
| Kin23 | <1 | 6 | 48 | <1 |
| Kin24 | <1 | 22 | 93 | <1 |
| Kin25 | <1 | 8 | 53 | <1 |
| Kin26 | 7 | <1 | 27 | 18 |
| Kin27 | <1 | <1 | 135 | 8 |
| Kin28 | 157 | 21 | 115 | 19 |
| Kin29 | 4 | 12 | 57 | < 1 |

Table 7
Perpendicular kinematics.

| Kinematics | $p_m$ [GeV/c] | $\sigma 5$ [b/GeV/sr] | Coinc. [1/hr] | Time [hr] | $\delta\sigma 5$ | $\delta R_{TL}$ | $\delta R_T$ | $\delta R_{L+TT}$ |
|---|---|---|---|---|---|---|---|---|
| Kin01 | 0.000 | 0.370E-05 | 0.377E+07 | 1.0 | <1% | N/A | 2.6% | 11.1% |
| Kin02 | 0.000 | 0.759E-07 | 0.252E+05 | 1.0 | <1% | | | |
| Kin03 | 0.100 | 0.184E-05 | 0.187E+07 | 1.0 | <1% | 9.7% | | |
| Kin04 | 0.100 | 0.131E-05 | 0.134E+07 | 1.0 | <1% | | | |
| Kin05 | 0.200 | 0.209E-06 | 0.211E+06 | 1.0 | <1% | 5.2% | | |
| Kin06 | 0.200 | 0.108E-06 | 0.109E+06 | 1.0 | <1% | | | |
| Kin07 | 0.300 | 0.234E-07 | 0.234E+05 | 1.0 | <1% | 3.9% | | |
| Kin08 | 0.300 | 0.894E-08 | 0.896E+04 | 1.0 | <1% | | | |
| Kin09 | 0.400 | 0.259E-08 | 0.256E+04 | 16. | <1% | 4.3% | 6.5% | 18.0% |
| Kin10 | 0.400 | 0.758E-09 | 0.749E+03 | 8.0 | 1% | | | |
| Kin11 | 0.400 | 0.376E-10 | 0.125E+02 | 46. | 4% | | | |
| Kin12 | 0.500 | 0.521E-09 | 0.507E+03 | 21. | <1% | 7.5% | 12.1% | 30.0% |
| Kin13 | 0.500 | 0.121E-09 | 0.117E+03 | 15. | 2% | | | |
| Kin14 | 0.500 | 0.719E-11 | 0.239E+01 | 64. | 8% | | | |

Table 8
High Missing Momentum.

| Kinematics | $p_m$ [GeV/c] | $\sigma 5$ [b/GeV/sr] | Coinc. [1/hr] | Time [hr] | $\delta\sigma 5$ |
|---|---|---|---|---|---|
| Kin15 | 600 | 0.127E-09 | 0.121E+03 | 4.0 | 4% |
| Kin16 | 750 | 0.167E-10 | 0.153E+02 | 10.0 | 8% |
| Kin17 | 800 | 0.164E-11 | 0.143E+01 | 16.0 | 20% |
| Kin18 | 1050 | 0.200E-12 | 0.163E+00 | 30.0 | 44% |
| Kin19 | 1200 | 0.186E-13 | 0.140E-01 | 40.0 | — |

Table 9
Parallel kinematics.

| Kinematics | $p_m$ [GeV/c] | $\sigma 5$ [b/GeV/sr] | Coinc. [1/hr] | Time [hr] | $\delta\sigma 5$ | $\delta R_T$ | $\delta R_L$ | $\delta R_L/R_T$ |
|---|---|---|---|---|---|---|---|---|
| Kin20 | 0.000 | 0.275E-04 | 0.163E+08 | 1.0 | <1% | 3.0% | 9.2% | 11.7% |
| Kin21 | 0.000 | 0.448E-06 | 0.142E+06 | 1.0 | <1% | | | |
| Kin22 | 0.000 | 0.637E-06 | 0.933E+06 | 1.0 | <1% | 3.2% | 27.5% | 30.4% |
| Kin23 | 0.000 | 0.392E-07 | 0.209E+05 | 1.0 | <1% | | | |
| Kin24 | 0.000 | 0.418E-07 | 0.871E+05 | 1.5 | <1% | 3.1% | 55.0% | 57.7% |
| Kin25 | 0.000 | 0.589E-08 | 0.322E+04 | 3.5 | <1% | | | |
| Kin26 | 0.300 | 0.667E-07 | 0.226E+05 | 10. | <1% | 5.4% | 16.6% | 23.3% |
| Kin27 | 0.300 | 0.185E-08 | 0.630E+03 | 20. | <1% | | | |
| Kin28 | -0.300 | 0.131E-06 | 0.112E+06 | 5. | <1% | 8.6% | 19.2% | 27.5% |
| Kin29 | -0.300 | 0.101E-07 | 0.449E+04 | 10. | <1% | | | |

### *5.4 Systematic and Statistical Uncertainties*

With careful luminosity monitoring and elastic cross section measurements at appropriate energies we should be able to achieve a systematic uncertainty of 2% as exhibited in the E89-044 experiment on $^3$He. We have therefore assumed a systematic uncertainty of 2% for all our cross section measuremets. In Tables 7, 8 and 9 the uncertainty in the five-fold differential cross sections, denoted as $\sigma 5$, includes only the statistical uncertainty, while the uncertainty for the response functions includes both statistical and systematic uncertainties.

In Fig. 6 and Fig. 7 the coincidence rate and the accidental rate is plotted for the parallel and perpendicular kinematics. Even for our most extreme kinematics the signal to accidental ratio is greater than one. Further, it is possible to reduce the accidentals by a factor of 5 by requiring a consistent vertex from both spectrometers and another factor of 10 from a missing mass cut.

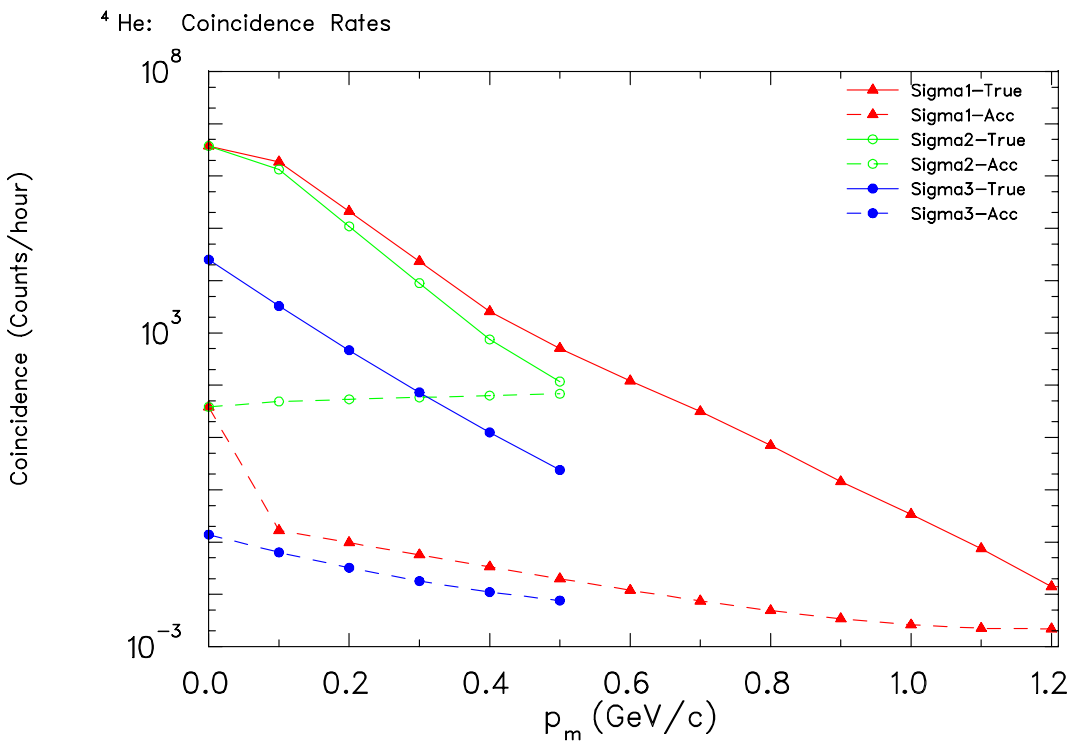


Fig. 6. The coincidence and accidental rates are shown for the perpendicular kinematics.

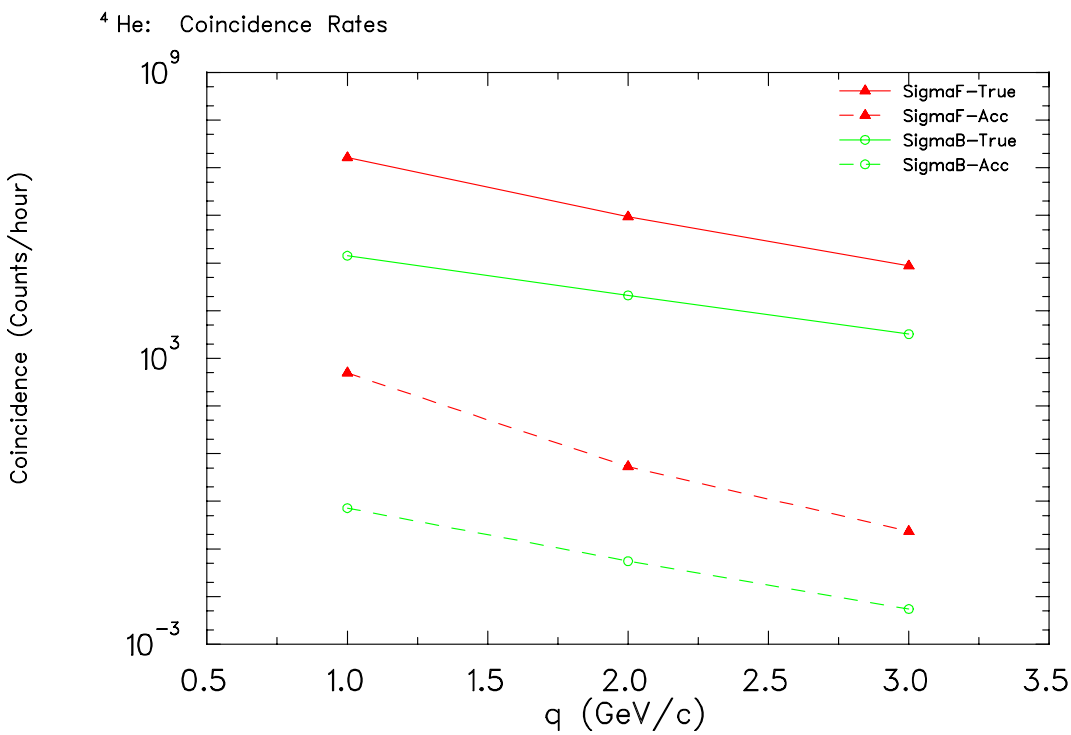


Fig. 7. The coincidence and accidentanl rates are shown for the parallel kinematics.

## 6 Theoretical Predictions

### *6.1 Relativistic Mean Field Calculation*

In the relativistic mean field calculations performed with the code provided by J.M. Udias [38], a bound state wave function is used that is the solution of the Dirac equation using standard Wood-Saxon (WS) wells for the scalar(S) and vector(V) potentials. The parameters of the WS potentials are fitted to the measured rms radius and binding energy of $^4$He. This reproduces quite well the $^4$He(e,e'p)$^3$H momentum distribution. A general solution of a bound particle using the Dirac equation has a different ratio of upper and lower components than for a free nucleon, that is, it always has a negative energy component. The spinors in a completely relativistic calculation are often referred to as "distorted" because of the presence of the scalar and vector potentials appearing in the lower component [13,39]. The positive energy projected solutions resemble free spinors containing only the usual terms connecting the upper and lower components, The Udias code calculates DWIA or PWIA always using relativistic kinematics. Proton distortions are calculated solving the Dirac equation using an optical potential. The only nonrelativistic option is to remove the relativistic dynamics from the wave functions, for either the bound state proton or continuum proton, by projecting out the negative energy components, but the operator and kinematics will still be fully relativistic. It is worth noting that the recent Hall A results for response functions and the $A_{TL}$ asymmetry from $^{16}$O(e,e'p)$^{15}$N [3] were well described by the full relativistic calculation of Udias [40,41].

### *6.2 Microscopic Calculation*

In the microscopic calculation performed with a code provided by J.-M. Laget, the reaction amplitude is expanded in diagrams which are computed in momentum space [16]. The code used the Urbana V14 potential. The diagrams for his Plane Wave Impuse Approximation, PWIA, calculation are shown in Fig. 8. The left diagram is the simplest Feynman diagram for the $^4$He(e,e'p)$^3$H reaction. In this figure the virtual photon couples to one-nucleon. In the right diagram, the recoil contribution is taking into account, i.e. when the virtual photon couple to the triton.

For the full calculations of J.-M. Laget, the two-body and three-body mechanisms are taken into account. The two-body diagrams are shown in Fig. 9. Here the two-nucleon meson exchange amplitudes are shown in a. and b. and the nucleon-nucleon rescattering is taken into account in diagrams c. and d. Both isospin states (T=0,1) of the initial nucleon pair are taken into account. In three-body diagrams are shown in Fig. 10. In these diagrams the recombination of the $^4$He breakup and the $^3$H recombination are taken into account.

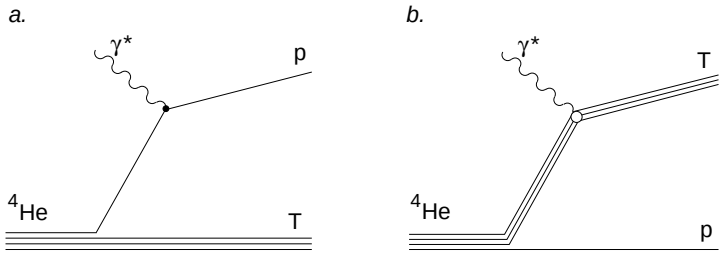


Fig. 8. The one-body mechanisms.

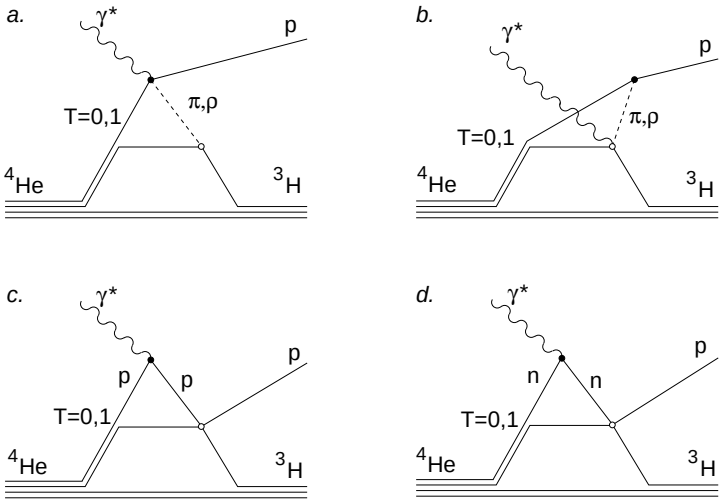


Fig. 9. The two-body mechanisms.

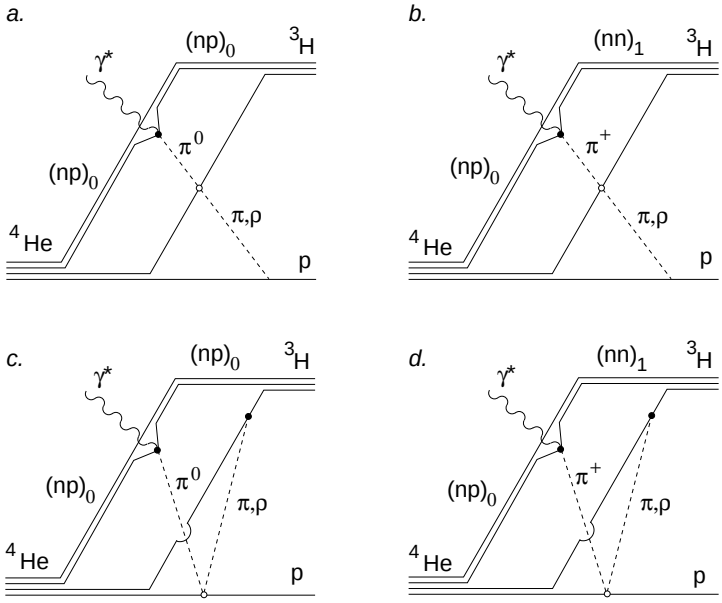


Fig. 10. The three-body mechanisms.

### *6.3 Theoretical Development*

Recently, S. Jeschonnek and R. Schiavilla have begun developing detailed calculations for $^3$He and $^4$He [42]. R. Schiavilla will provide the bound state wave function using the Argonne V18 potential [35]. S. Jeschonnek will introduce the relativistic current operator, as she has already done for the deuteron [43]. This operator can now be applied to any target nucleus [42]. S. Jeschonnek will also include Final State interactions with the Glauber approximation [44]. When combined, this should provide the most realistic theoretical model for the recent $^3$He(e,e'p) experiment and for this proposed $^4$He(e,e'p) measurement. This calculation will be developed over the course of the next several months.

## 7 Expected Results

On the following pages the expected results from the proposed measurements is shown along with the calculations of J.M. Udias and J.M. Laget. The shaded region on the figures indicates the range in $p_m$ for which $R_{TL}$, $R_T$, and $R_{L+TT}$ will be extracted. Figures 11, 12, and 13 show the expected cross section results, figure 14 shows the expected $A_{TL}$ results, and figures 15, 16, and 17 show the expected response function separation results.

In the figures, the Udias-RDWIA curves corresponds to the fully relativistic calculation described in section 6.1. The RPWIA curves are also a fully relativistic calculation, but with the outgoing proton treated as a free Dirac particle, i.e. no distortions and no negative energy components. The bound state, however, is still treated as a bound Dirac particle, so it still contains negative energy components. For the Udias-EMAnoSV curves the negative energy components of the bound proton and outgoing proton are projected out and only the positive energy components are used, and outgoing proton is treated as a plane wave Dirac spinor. Also the effective momentum approximation (EMA) with no spinor distortion (no SV) is used, which means the bound proton and continuum proton have the same upper/lower spinor component ratios as for free particles and that asymptotic values of the momenta are used. The Laget-Full curves includes all two- and three-body mechanisms described in section 6.2 while the Laget-PWIA curves includes only the one-nucleon exchange amplitude.

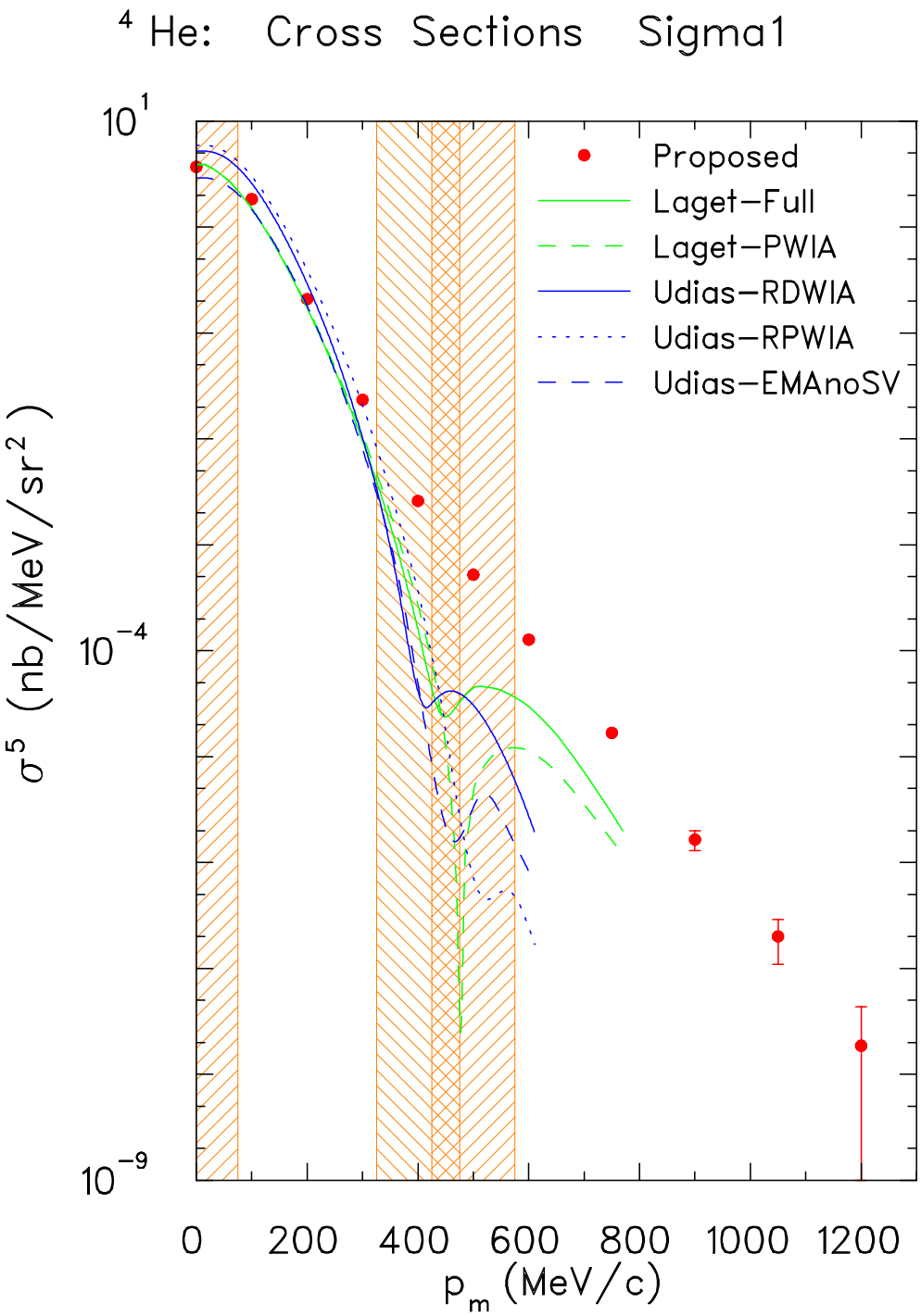


Fig. 11. The expected data is shown for the perpendicular kinematics, $\mathbf{q}$ = 1.5 GeV/c and $\omega$ = 0.84 GeV, with $\epsilon$ = 0.943 and $\phi$ = 180°. In this kinematics, denoted as $\Sigma 1$, the data up to 0.50 GeV/c will be used to determine the $R_{TL}$, $R_T$, and $R_{L+TT}$ response function separations and to extract the $A_{TL}$ asymmetry, while the higher $p_m$ data will be used solely as a cross section measurement.

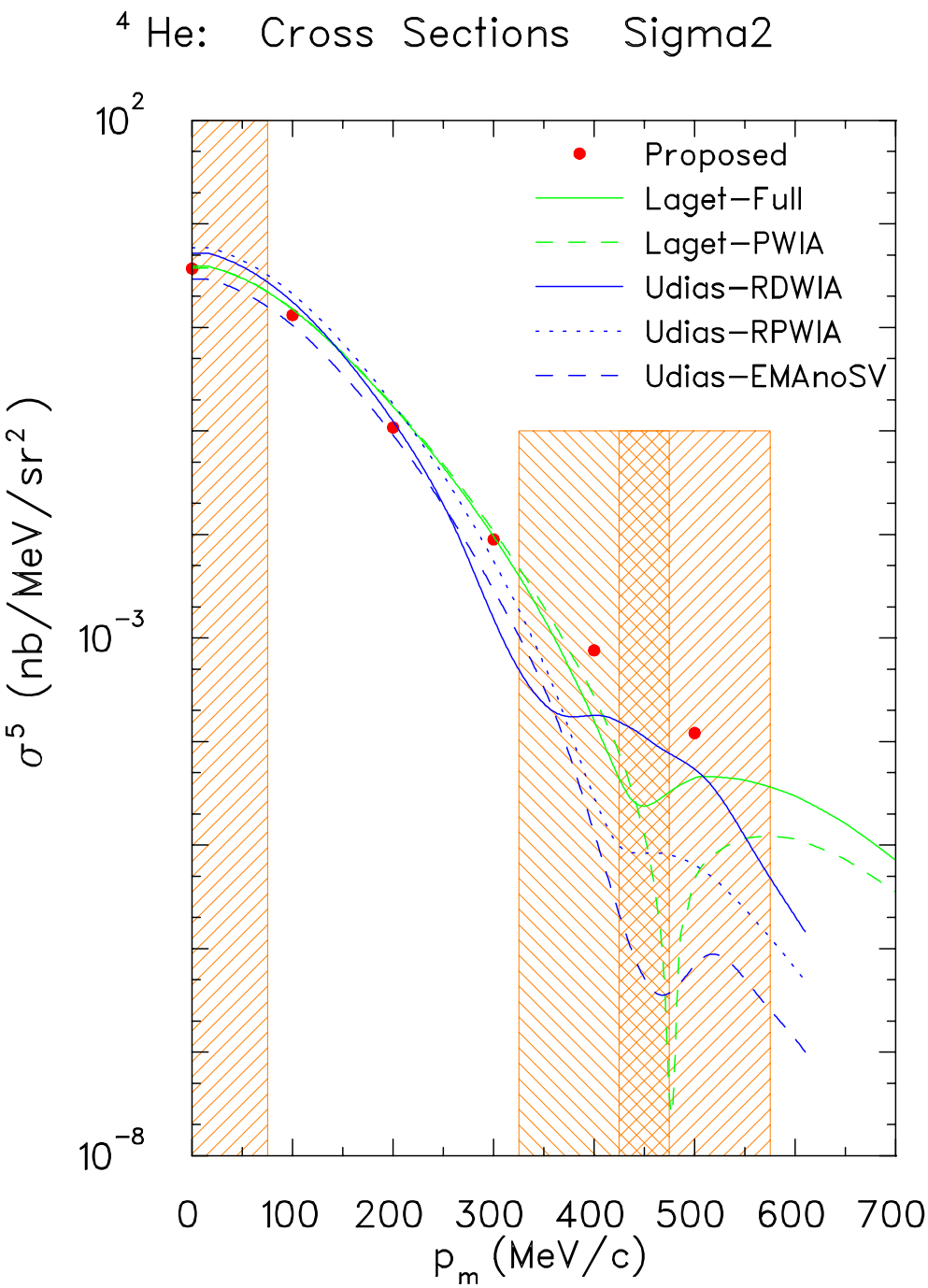


Fig. 12. The expected data is shown for the perpendicular kinematics, $\mathbf{q} = 1.5$ GeV/c and $\omega = 0.84$ GeV, with $\epsilon = 0.943$ and $\phi = 0°$. In this kinematics, denoted as $\Sigma 2$, the data will be used for the $R_{TL}$, $R_T$, and $R_{L+TT}$ response function separations and to extract the $A_{TL}$ asymmetry.

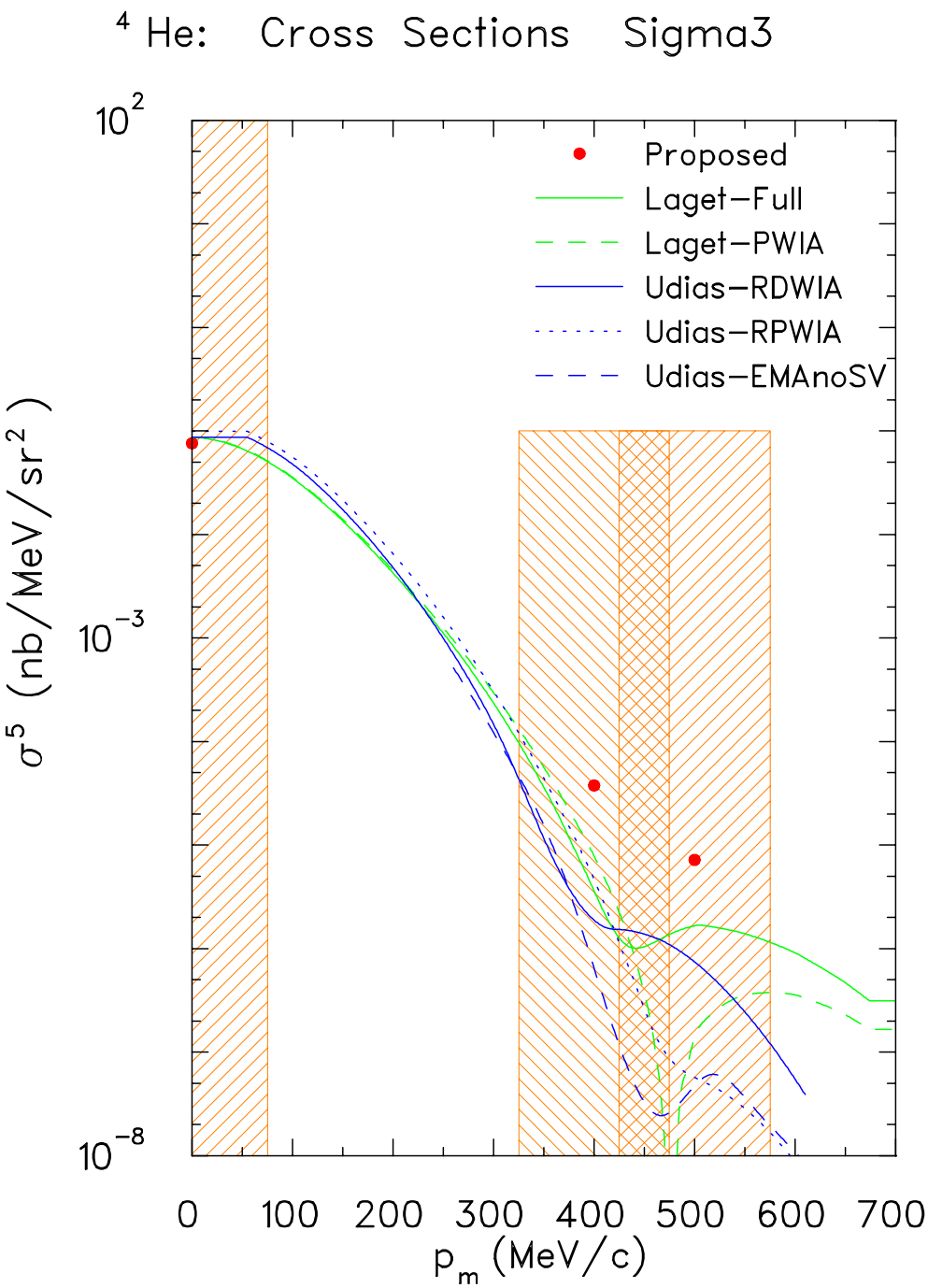


Fig. 13. The expected data is shown for the perpendicular kinematics, $\mathbf{q} = 1.5$ GeV/c and $\omega = 0.84$ GeV, with $\epsilon = 0.108$ and $\phi = 180°$. These data points will be used in order to make the $R_T$ and $R_{L+TT}$ separations.

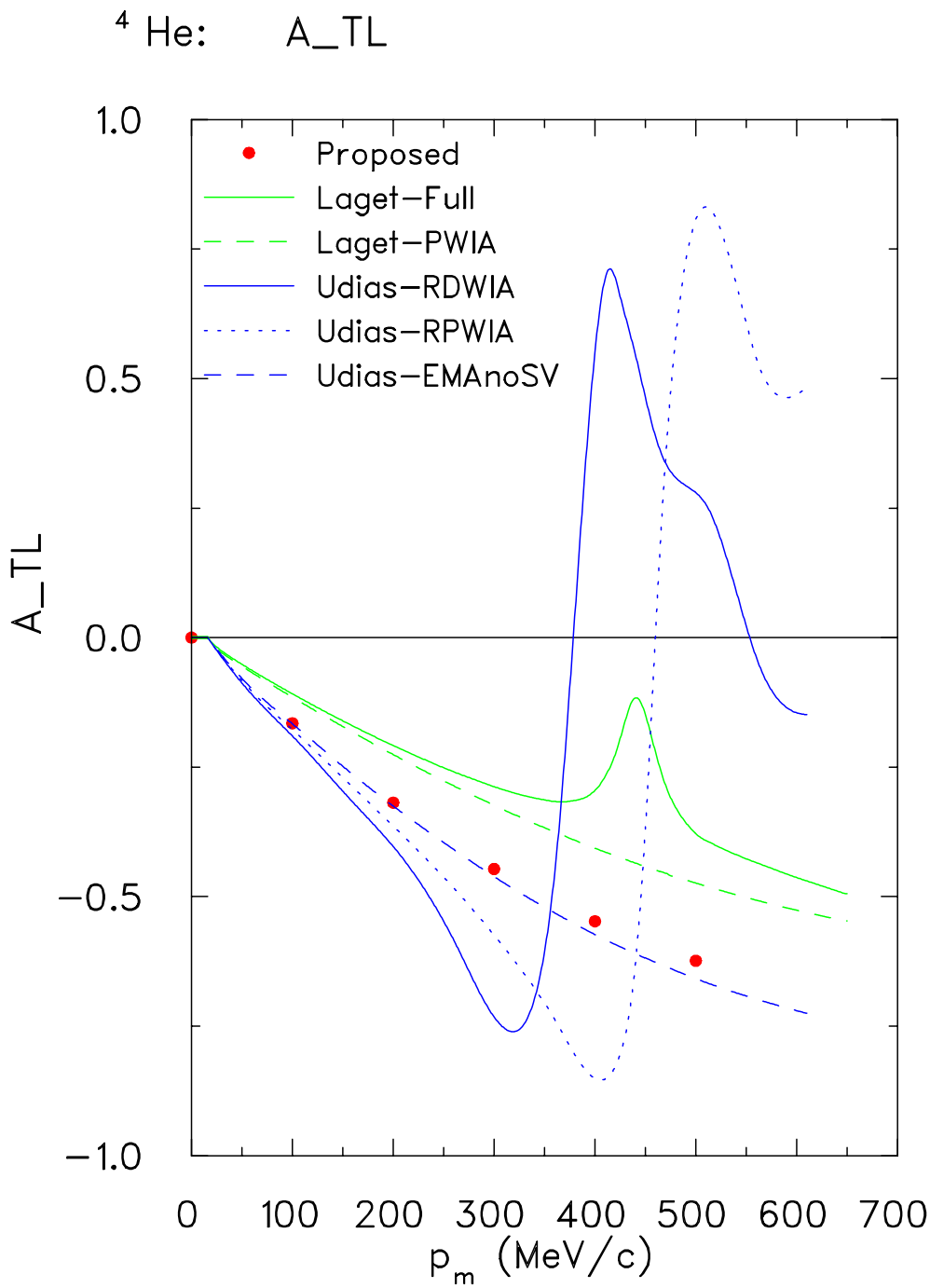


Fig. 14. Shown is the expected $A_{TL}$ asymmetry extracted from the $\Sigma 1$ (see figure 11) and $\Sigma 2$ (see figure 12) cross section measurements. Both the full calculations of J.M. Udias and J.-M. Laget predict this asymmetry to be very sensitive to the "dip" in the PWIA cross section. It is worth noting, that in PWIA the calculations show $A_{TL}$ to be completely insensitive to the dip.

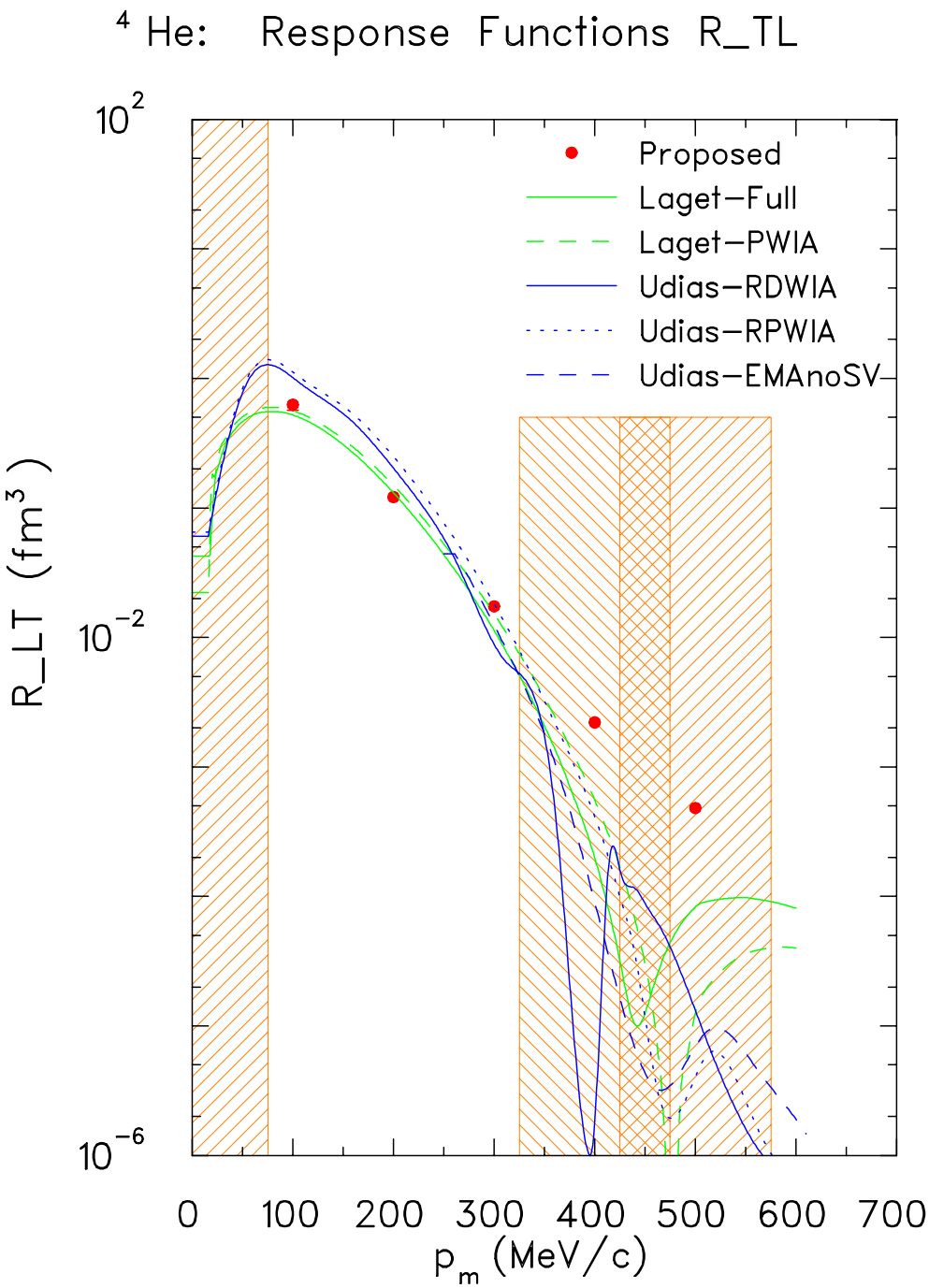


Fig. 15. Shown is the expected result of $R_{TL}$ response functions determined using the cross sections from $\Sigma 1$ (see figure 11) and and $\Sigma 2$ (see figure 12) kinematics.

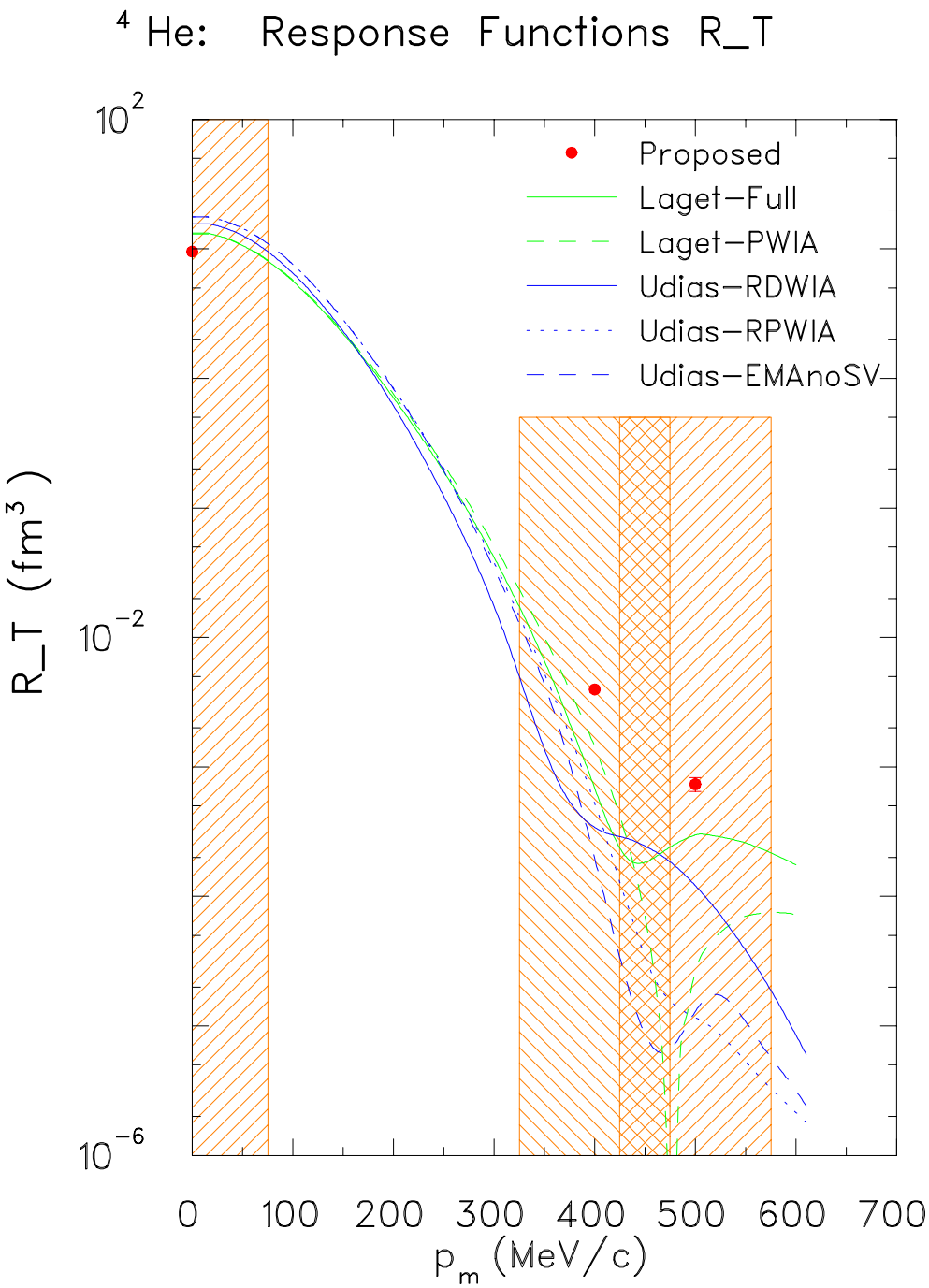


Fig. 16. Shown is the expected result of $R_T$ response function separations determined using the cross sections from $\Sigma 1$ (see figure 11) and from $\Sigma 3$ (see figure 13) kinematics.

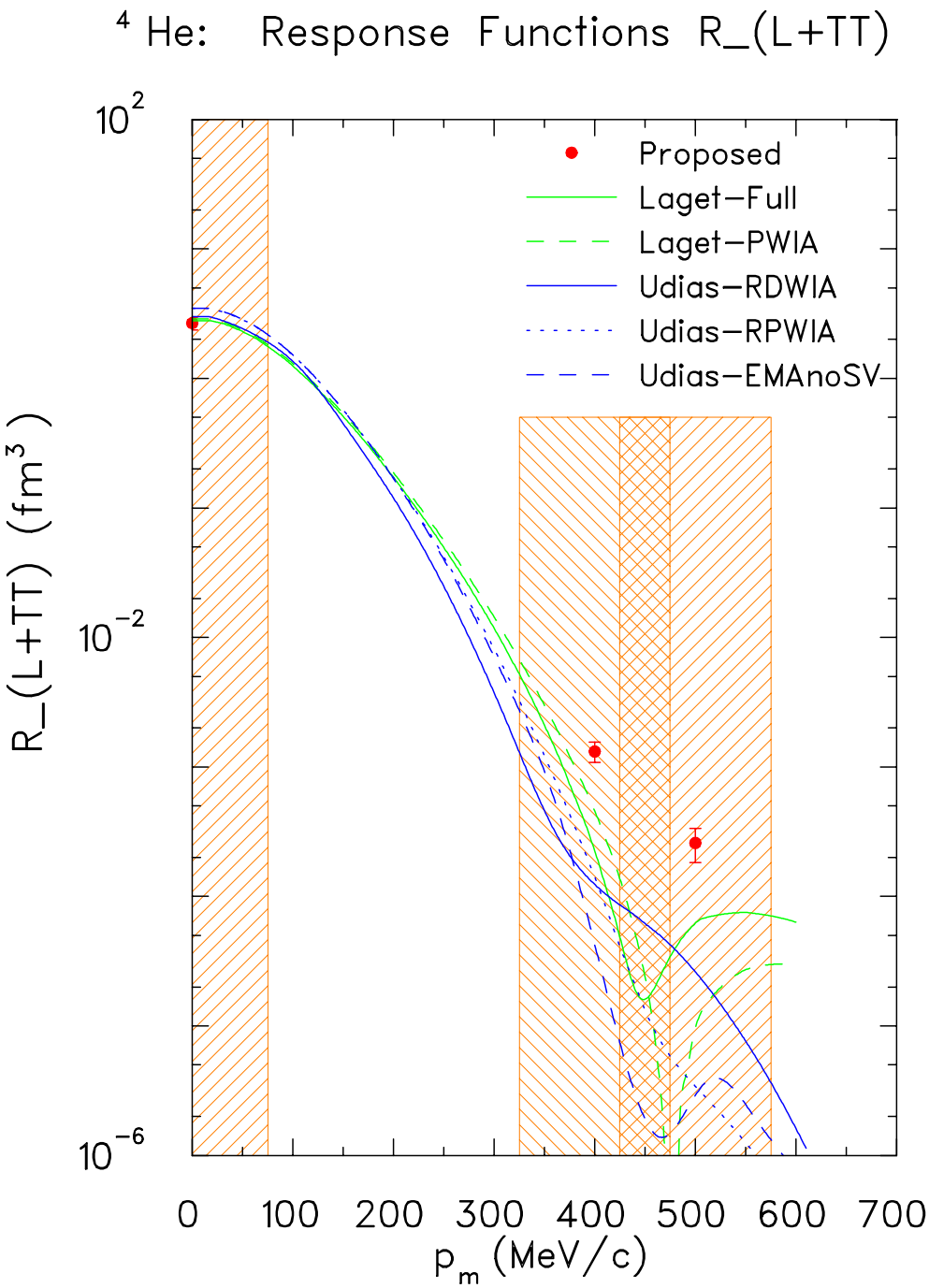


Fig. 17. Shown is the expected result of $R_{L+TT}$ response function separations determined using the cross sections from $\Sigma 1$ (see figure 11) and from $\Sigma 3$ (see figure 13) kinematics.

## 8 Beamtime Request

To perform this experiment and make the necessary systematic measurements, we request 20 days of beamtime, as shown in Table 10. The time estimates in Tables 7, 8, and 9 have been adjusted up by 30% to account for radiative losses. The table shows all necessary time, including the time to move the spectrometers. The different energies needed by this experiment only require a different pass beam to be sent to Hall A, except for the 1.25 GeV beam.

Table 10
Time requested for the $^4$He(e,e'p)$^3$H response function seperation experiment.

| | |
|---|---|
| Cross Section Measurements | 424 hrs |
| Spectrometer Field and Position Changes | 16 hrs |
| ARC and EP Energy Measurements | 12 hrs |
| Carbon Pointing and Optics Measurements | 16 hrs |
| Elastic Scattering Measurements | 12 hrs |
| Total | 480 hrs (20 days) |

We will preform these ARC and EP energy measurments for each beam energy. Each measurment take approximately one hour, therefore we request 12 hrs to perform these measurements. For each position of the spectrometers, we will take carbon pointing data. For these measurements we measure $^{12}$C(e,e') and $^{12}$C(e,p) from a multifoil carbon target. This allows us to calibrate the pointing of the spectrometers for each kinematics. This method has shown itself to agree with survey data while taking less time. These measurments take approximately 1/2 hour each and we therefore request 16 hrs to perform them.

The final item is performing elastic scattering measurments. By making measurements of the well known elastic scattering, we are able to check our knowledge of the target thickness. When preforming an elastic $^4$He(e,e') measurement, the hadron spectrometer is placed at an angle for an upcoming $^4$He(e,e'p) kinematics. By continously monitoring the singles rates and only moving one spectrometer at a time, we have continuous monitoring of the target thickness which links back to the elastic measurment. Only for the highest beam energy is this technique not viable, since the Hall A electron spectrometers can only achieve momenta of approximately 4.2 GeV/c. For this particular case, we measure elastic scattering from the target with a lower beam energy immediately before and after the 4.8 GeV/c run period. By monitoring the tempurature and pressure of the target during the energy change, we can account for target density changes, although during the E89-044 experiment no changes were observed in temperature and pressure for long periods of time and the elastic scattering measurements taken before and after the 4.8 GeV/c run period both produced the same result. For these measurments we request 16 hours.

## References


[1] J.J. van Leeuwe, Ph.D. thesis, Universiteit Utrect (1996).

[2] J.J. van Leeuwe *et al.*, Phys. Rev. Lett. **80** (1998) 2583.

[3] J. Gao *et al.*, Phys. Rev. Lett. **84** (2000) 3265.

[4] J. Templon *et al.*, Systematic Probe of Short-Range Correlations via the Reaction $^4$He(e,e'p)$^3$He, TJNAF Hall A Proposal E97-111.

[5] J-E. Ducret *et al.*, Nucl. Phys. **A556** (1993) 373.

[6] Z.-E. Mezianni *et al.*, Nucl. Phys. **A553** (1993) 701c.

[7] J-E. Ducret *et al.*, Nucl. Phys. **A553** (1993) 697c.

[8] J.W. van Orden, N. Devine and F. Gross, Phys. Rev. Lett. **75** (1995) 4369.

[9] E. Hummel and J.A. Tjon, Phys. Rev. C **49** (1994) 21.

[10] J. Golak *et al.*, Phys. Rev. **C51** (1995) 1638.

[11] R. Schiavilla, V. Pandaripande and R. Wiringa, Nucl. Phys. **A449** (1986) 219.

[12] R. Schiavilla, Phys. Rev. Lett. **65** (1990) 835.

[13] J.M. Udias *et al.*, nucl-th/0101038v2.

[14] V.D. Efros, W. Leidemann and G. Orlandini, Phys. Rev. C **58** (1998) 552.

[15] Z. Zhou *et al.*, nucl-ex/0105006.

[16] J.M. Laget, Nucl. Phys. **A579** (1994) 333.

[17] S.I. Nagorny *et al.*, Sov. J. Nucl. Phys. **49** (1989) 465.

[18] S.I. Nagorny *et al.*, Sov. J. Nucl. Phys. **53** (1991) 228.

[19] M.B. Epstein *et al.*, Phys. Rev. Lett. **70** (1993) 2868.

[20] J.M. Laget, Nucl. Phys. **A497** (1989) 391c.

[21] R.E.J. Florizone, Ph.D. thesis, Massachusetts Institute of Technology (1999).

[22] A.A. Kozlov, Ph.D. thesis, University of Melbourne (2000).

[23] A.A Kozlov *et al.*, Nucl. Phys. **A684** (2001) 460.

[24] T. de Forest, Nucl. Phys. **A392** (1983) 232.

[25] J.J. van Leeuwe *et al.*, Nucl. Phys. **A631** (1998) 593c.

[26] N. Liyanage *et al.*, to be published in Phys. Rev. Lett. (2001), nucl-ex/0009017.

[27] J Ryckebusch *et al.*, Nucl. Phys. **A624** (1997) 581.

[28] J.M. LeGoff *et al.*, Phys. Rev. **C50** (1994) 2278.

[29] M.B. Epstein, A. Saha, R. Lourie and J. Mougey, Selected Studies of the $^3$He and $^4$He Nuclei through Electrodisintegration at High Momentum Transfer, TJNAF Hall A Proposal E89-044.

[30] W Bertozzi, K. Fissum, A. Saha and L. Weinstein, Testing the Limits of the Single Particle Model in $^{16}$0(e,e'p): an update to e89003, TJNAF Hall A Proposal E00-102.

[31] B. Hersman, Update on CEBAF Proposals PR-89-015, -017, -027, -031, -32, and -036, TJNAF Hall B Proposal E91-009.

[32] L. Weinstein, W. Bertozzi and W. Boeglin, Coincidence Reaction Studies with the LAS, TJNAF Hall B Proposal E89-027.

[33] R.E.J. Florizone *et al.*, Phys. Rev. Lett. **83** (1999) 2308.

[34] J. F. J. van den Brand *et al.*, Nucl. Phys. **A534** (1991) 637.

[35] R.B. Wiringa, V.G.J. Stoks and R. Schiavilla, Phys. Rev. C **51** (1995) 38.

[36] J.W. Lightbody and J.S. O'Connel, Computers in Physics, May/June (1988) 57.

[37] A. Saha, Private communication.

[38] J.M. Udias, Private communication.

[39] J.J. Kelly, Phys. Rev C **60** (1999) 044609.

[40] J. M. Udias, J. A. Caballero, E. Moya de Guerra, J. E. Amaro and T. W. Donnelly, Phys. Rev. Lett. **83** (1999) 5451.

[41] J.M. Udias *et al.*, Phys. Rev. C **51** (1995) 3246.

[42] S. Jeschonnek and R. Schiavilla, Private communication.

[43] S. Jeschonnek and T.W. Donnelly, Phys. Rev. C **57** (1998) 2438.

[44] S. Jeschonnek and T.W. Donnelly, Phys. Rev. C. **59** (1999) 2676.